ISSN 8755-6839

SCIENCE OF TSUNAMI HAZARDS

Journal of Tsunami Society International

Volume 30 Number 3 2011

DETECTION OF LOCAL SITE CONDITIONS INFLUENCING EARTHQUAKE SHOCK AND SECONDARY EFFECTS IN THE VALPARAISO AREA IN CENTRAL-CHILE USING REMOTE SENSING AND GIS METHODS

Barbara Theilen-Willige [1] **and Felipe Barrios Burnett** 2

[1] TU Berlin, Institute of Applied Geosciences, Berlin, Germany, E-mail: Barbara. Theilen-Willige@t-online.de

[2] Hydrographic and Oceanographic Service of the Chilean Navy, Department of Hydrography, and E-mail: fbarrios@shoa.cl

ABSTRACT

The potential contribution of remote sensing and GIS techniques to earthquake hazard analysis was investigated in Valparaiso in Chile in order to improve the systematic, standardized inventory of those areas that are more susceptible to earthquake ground motions or to earthquake related secondary effects such as landslides, liquefaction, soil amplifications, compaction or even tsunami-waves. Geophysical, topographical, geological data and satellite images were collected, processed, and integrated into a spatial database using Geoinformation Systems (GIS) and image processing techniques. The GIS integrated evaluation of satellite imageries, of digital topographic data and of various open-source geodata can contribute to the acquisition of those specific tectonic, geomorphologic/ topographic settings influencing local site conditions in Valparaiso, Chile. Using the weighted overlay techniques in GIS, susceptibility maps were produced indicating areas, where causal factors influencing near-surface earthquake shock occur aggregated. Causal factors (such as unconsolidated sedimentary layers within a basin's topography, higher groundwater tables, etc.) summarizing and interfering each other, rise the susceptibility of soil amplification and of earthquake related secondary effects. This approach was used as well to create a tsunami flooding susceptibility map. LANDSAT Thermal Band 6-imageries were analysed to get information of surface water currents in this area.

Key Words: *Local site conditions, tsunami and slope failure susceptibility, Central-Chile, remote sensing and GIS*

Science of Tsunami Hazards, Vol. 30, No. 3, page 191 (2011)

1. INTRODUCTION

The Chilean subduction zone has one of the highest levels of seismic activity in the world. Large mega-earthquakes of magnitudes >8 occur on the average every 5–10 years (Table 1). These earthquakes result from the on-going active subduction of the Nazca plate beneath South America (Vigny et al., 2009). Preparing for such mega-earthquakes requires a long-term public policy in enforcing building regulations (Madariaga et al., 2010). When planning and rebuilding in earthquake prone areas, local site conditions that influence earthquake ground motions need to be carefully evaluated. For earthquake disaster preparedness, it is helpful to know which areas might be more susceptible to ground motions and secondary effects and distinguish them from areas affected by specifically by local site conditions.

Table 1. Earthquakes with Magnitudes >7 according to Winckler-Grez & Vásquez-Álvarez (2008) and USGS (2010)

Year	Length (km)	Width (km)	Displacement (m)	Ml
1575				7.0 – 7.5
1647	365			8.5
1730	350 – 550	100-150	6 - 8	8.75
1822	200 – 330	100-150	3 - 6	8.5
1906	365 – 330	100-150	3 - 6	8.2 – 8.3
1985	170	100	1.23 – 2.80	7.8
2010	550	100	3 - 4	8.8

Local geologic conditions are the cause of differences in earthquake intensity. However, particular conditions of specific areas and the degree to which are they affected by the earthquake's ground motions are often the main cause of intensity variations.
Earthquake ground motions depend primarily on such factors as the quake's magnitude, the physical properties of the strata along the rupture zone, the distance from the fault and the local geologic conditions. The most intense shaking generally occurs near the rupturing fault area and decreases with distance. However, the ground motions at one site can be stronger than at another site, regardless of the distance (Gupta, 2003).

The variability in earthquake-induced damage is mainly determined by the local lithologic and hydro-geological conditions. These conditions, in turn influence the amplitude, the frequency and duration of ground motion at a site. Flat areas (below 10° slope gradient) within morphologic basins and depressions are usually covered by younger, unconsolidated sediments. Ground with high liquefaction or compaction response is occurs in areas with newly formed sediments. Soft soils can amplify shear waves and, thus, amplify ground shaking. Unconsolidated sediments slow the earthquake wave velocity, trapping the energy and thus causing more intense shaking. Newer sediments near a source of water often contain water-filled pore spaces. As earthquake's energy cyclically compresses these sediments, the pore pressure in the pore spaces

increases to a level greater than the confining pressure of the soils above them, causing small geyser-like sand boils that spew water and sand and result in ground subsidence. If buildings and other structures sit atop these hazardous areas, they have a higher risk of damage or collapse.

The fundamental phenomenon responsible for the amplification of motion over soft sediments is the trapping of seismic waves due to the impedance contrast between sediments and underlying bedrock. When the structure is horizontally layered, this trapping affects body waves, which travel up and down in the surface layers. When lateral heterogeneities are present (such as thickness variations in sediment-filled valleys), this trapping also affects the surface waves, which develop on these heterogeneities. The interferences between these trapped waves lead to resonance patterns, the shape and the frequency of which are related with the geometrical and mechanical characteristics of the structure (Ehret & Hannich, 2004).

Groundwater level variations and associated saturation changes in sand layers within near-surface aquifers can influence local response spectra of the ground motion, through modification of shear-wave velocity. Wetlands generally have a higher damage potential during earthquakes due to longer and higher vibrations. Recently formed sediments will slow the velocity of the earthquake waves, trapping the energy and causing large amplitudes of shaking. Older compacted materials that over time have densified or transitioned from sand to sandstone and cemented together are less responsive for example to liquefaction. Changes of the groundwater level can have a considerable influence upon the liquefaction potential of a region due to in-situ pore-water pressure responses in aquifers during earthquakes triggering mechanism of liquefaction (Hannich et al., 2006). Liquefaction that affects the human-built environments is mostly limited to the upper 15 meters of soil.

Due to seasonal and climatic reasons a stronger earthquake during a wet season will probably cause more secondary effects than during a dry season. In very hot and dry seasons the risk of liquefaction or landslides is generally lower than in spring times. These seasonal effects should be monitored systematically.

Earthquakes cause damage to buildings and other structures both in near and far fields. This phenomenon of far field damages to buildings has been reported, worldwide, notable being the 1985 Mexico earthquake, where the epicenter was 400 km offshore from the Mexico city, which suffered very heavy damage (Steinwachs, 1988). This observation emphasizes the importance of local site conditions in either reducing or enhancing the earthquake hazard in a region.

Maps of seismic site conditions on regional scales require substantial investment in geological and geotechnical data acquisition and interpretation. Macroseismic maps that can help to detect local site conditions in Chile are based on different standards and scales (Ceresis, 1985). There is a strong need to improve the systematic, standardized inventory of areas that are more susceptible to earthquake ground motions or to earthquake related secondary effects such as landslides, liquefaction, soil amplifications, compaction or tsunami-waves. Therefore a uniform data base with a common set of strategies, standards and formats should be implemented.

Topographic variations can be considered as an indicator of near-surface lithology to the first order; with steep mountains indicating rock, nearly flat basins indicating soil, and a transition between the end members on intermediate slopes. In the seismically active region of Haiti, information about surficial geology and shear-wave velocity (*V*S) either varies in quality, varies spatially, or is not accessible. The similarity between the topography and the surficial site condition map, derived from geology is striking. Therefore the service provided by the USGS providing V_s^{30} data from all over the earth's surface based on these correlations (Wald & Trevor, 2007, USGS Seismic Hazard Program, Global V_s^{30} Map Server) was used for these investigations in Central-Chile.

1.2. Aim of study

The main objective of this study is to investigate the potential contribution of remote sensing and GIS techniques for the detection of areas more susceptible to earthquake ground motions due to local site conditions. The evaluation of satellite imageries and of digital topographic data is of great importance since it contributes to the acquisition of the specific geomorphologic/topographic settings of earthquake hazard affected areas by extracting geomorphometric parameters based on Digital Elevation Model (DEM) data. As digital elevation data acquired by SRTM (Shuttle Radar Topography Mission, 90m spatial resolution) and ASTER-data (30 m resolution, interpolated up to 15 m) are readily and freely available, so the standardized approach described in this paper can be utilized worldwide.

2. GEOLOGIC, SEISMOTECTONIC AND GEOMORPHOLOGIC SETTING

The study area along Central Chile is a segment of one of the longest coherent subduction zones known worldwide. This convergent plate margin has been created by the collision of the oceanic Nazca plate with the continental South American plate. The main characteristic features generated by the conversion are the deep-sea trench (having a maximum depth of 8000 m along the west front of the study area), the Wadati Benioff Zone (WBZ) and the impressive Andean orogen. The shallow part of the WBZ - which hosts the seismogenic zone - has a dip angle of approximately 20◦ (Sobiesiak, 2004). The Nazca plate moves towards the South American plate at a rate of about 7 cm/year. Along this fault zone, the Nazca plate dives into the earth's mantle. Because of the rapid convergence, the Chilean subduction has strong seismic activity, with earthquakes of magnitude 8 occurring every decade on the average. One earthquake of M > 8.7 occurs at least every century. In addition, the largest earthquake ever recorded in recorded history (Mw 9.4-9.5) occurred in 1960, just south of Concepcion in Central Chile (Vigny, 2010). Fig.1 shows earthquake epicenters and documented tsunami events in Central Chile. Fig. 2 provides a LANDSAT 3D-overview of the geomorphologic setting, showing mountainous areas subdivided by elongated valleys, broader basins and coastal lowlands covered by unconsolidated, Quaternary sediments.

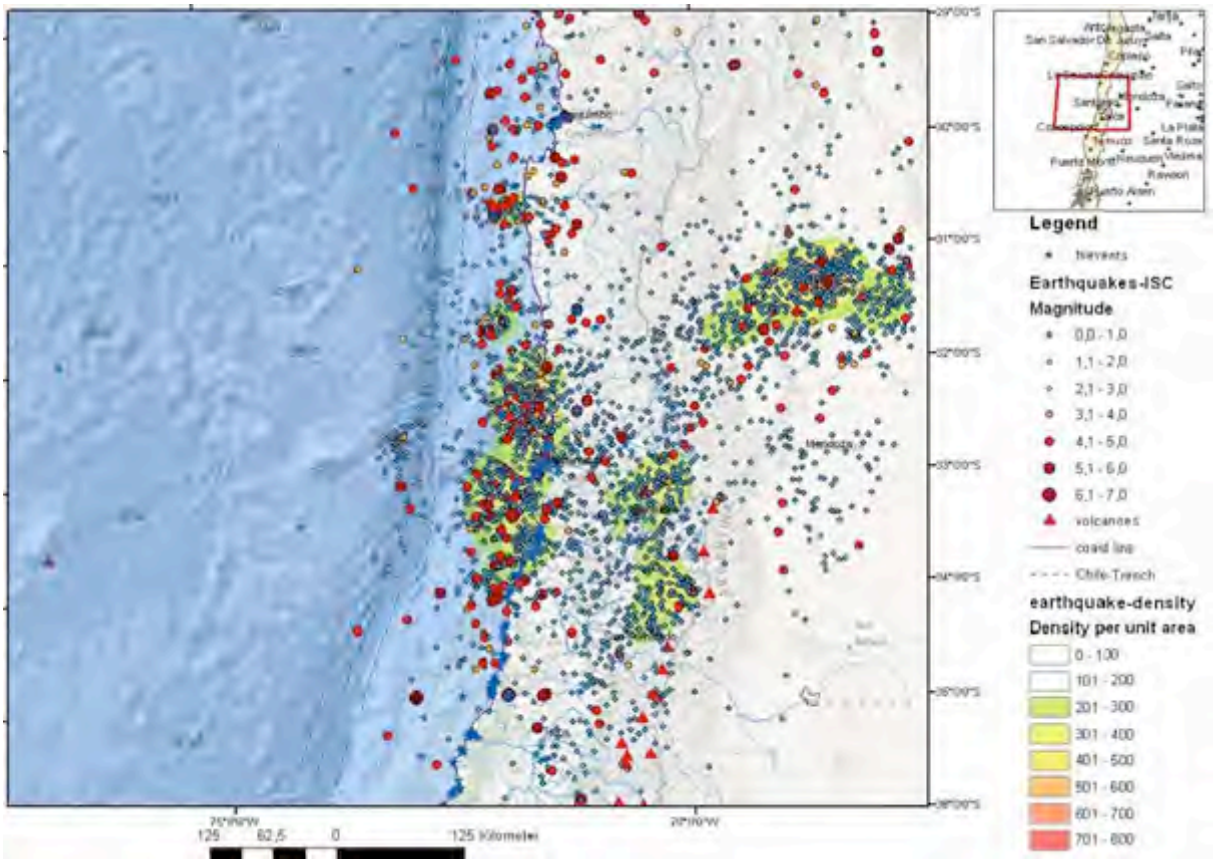

Fig.1. Earthquakes in Central-Chile (Earthquake data: USGS, ISC, NOAA, GFZ)

3. METHODS

GIS integrated geodata analysis can be used to detect, map and visualize factors that are known to be related to the occurrence of higher earthquake shock and / or earthquake induced secondary effects: factors such as lithology (loose sedimentary covers), basin and valley topography, fault zones or steeper slopes.

3.1. Evaluations of morphometric maps derived from Digital Elevation Data (DEM)

Morphometric maps such as slope, hillshade, height level, and curvature maps are generated based on SRTM and ASTER Digital Elevation Model (DEM) data using ArcGIS from ESRI and ENVI digital image processing software (ITT). Step by step factors can be extracted from these data that might be of importance for the detection of local site conditions. For example: The distribution of unconsolidated, youngest sedimentary covers can often be correlated with areas showing less than 10° slope gradient and no curvature (in the case of the curvature: negative curvatures represent concave,

zero curvature represent flat and positive curvatures represents convex landscapes). Height level maps help to search for topographic depressions covered by recently formed sediments, which are usually linked with higher groundwater tables. When extracting the lowest height levels of an area, it becomes visible where the areas with high ground-water tables can be expected (Fig. 3). When earthquakes occur such areas have often shown the highest damage intensities (Schneider, 2004).

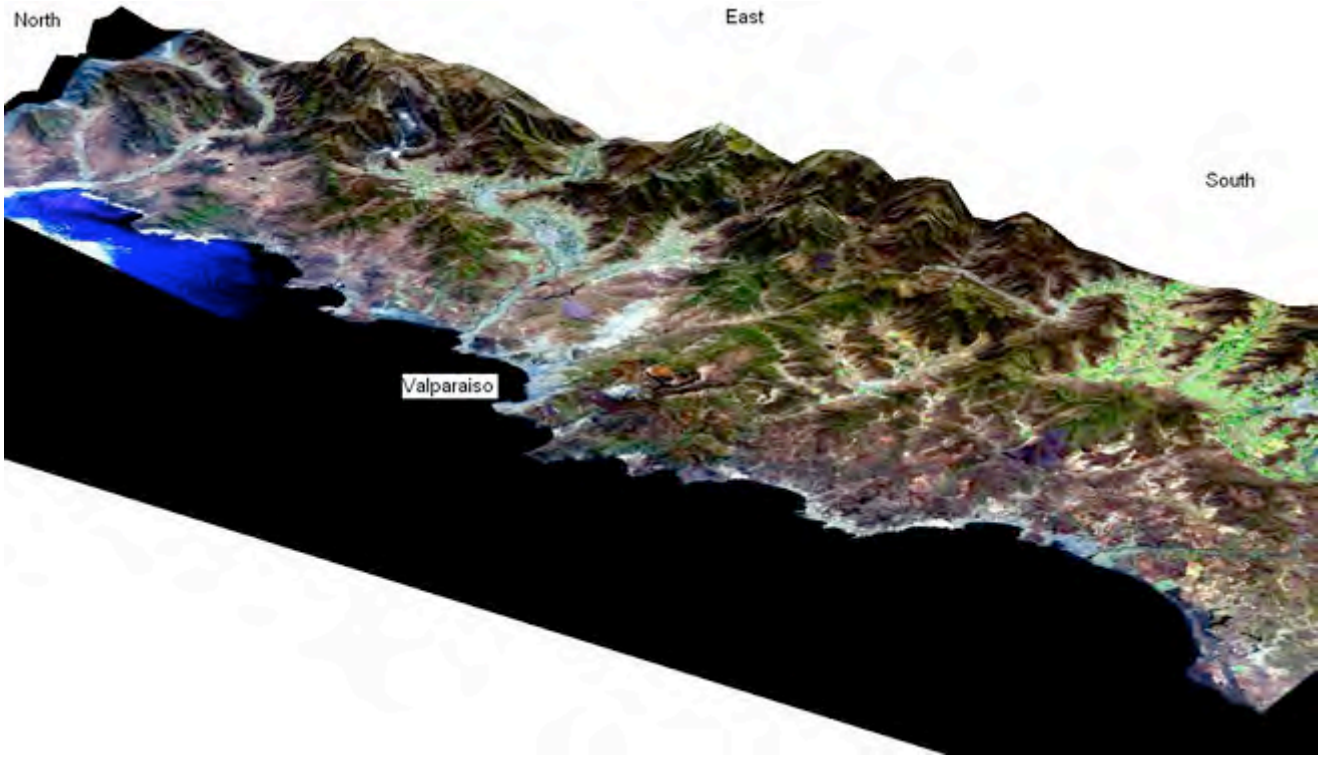

Fig. 2. Perspective 3D-view of a LANDSAT ETM image of the Valparaiso area merged with ASTER DEM data looking to the east

Slope gradient maps help detect areas where mass movements are likely to occur. Extracted from slope gradient maps are the areas with the steepest slopes and from curvature maps the areas with the highest curvature - as these are susceptible to landslides. Slopes with higher slope gradient (> 30°) are generally more susceptible to mass movements. By combining some of the causal or preparatory factors influencing earthquake shock intensity in a geo-referenced GIS environment, those areas can be detected where causal factors occur cumulatively and superimposed on each other. From SRTM and ASTER DEM data derived causal factors can be extracted such as:

- lowest *height levels* providing information of areas with relatively higher groundwater tables (here: 0-20 m),
- lowest *slope gradients* (< 5°-15°),

- lowest *minimum curvature or no curvature*, providing information of flat, broader valleys, basins and depressions with younger sedimentary covers and higher groundwater tables,
- highest *flow-accumulations,* providing information of areas with higher surface water-flow input, are combined with lithologic and seismo-tectonic information in a GIS data base as
- from geologic maps derived Quaternary sediment distributions and faults,
- from LANDSAT ETM imageries derived lineaments,
- from International Earthquake Centres downloaded earthquake data (International Seismological Centre, ISC, USGS, GFZ, etc.).

Causal or preparatory factors are extracted systematically in ESRI Grid-format. Of course, many further factors and data play an important role that - if available - should be included into the database.

The different factors are converted into ESRI-GRID-format and summarized/aggregated and weighted in % in the weighted overlay-tool of ArcGIS (Figs. 5 and 6) according their estimated influence on the local specific conditions or in equal percentages. Those areas are considered to be susceptible more to soil amplification of seismic waves where the following causal factors are summarizing and aggregating their effects: a) lowest height level of the terrain combined with relative high groundwater tables, b) flat morphology with low slope gradients and no curvature and c) loose sedimentary covers within a basin topography or within flat coastal areas. When an area is underlain by larger, active fault zones, especially when intersecting each other, the soil amplification susceptibility will probably rise, depending on given specific earthquake properties and parameters.

The percentage of influence of one factor is changing, as for example due to seasonal and climatic reasons, or distance to the earthquake source. As a stronger earthquake during a wet season will probably cause more secondary effects such as landslides or liquefaction than during a dry season, the percentage of its influence has to be adapted. Therefore the percentage of the weight of the different factors has to be adjusted as well to seasonal effects.

The sum over all factors / layers that can be included into GIS provides some information of the susceptibility in the amplification of seismic ground motions. After weightening (in %) the factors according to their probable influence on ground shaking susceptibility, maps can be elaborated, where those areas are considered as being more susceptible to higher earthquake shock intensities, where "negative" factors occur aggregated and interfering with each other. Whenever an earthquake occurs in these areas, now it can be derived better where the "islands" of higher ground shaking are most likely to occur by adding the specific information of the earthquake to the susceptibility map using the weighted overlay - approach.

The approach presented here is proposed to serve as a first basic data stock for getting a perception of potential sites susceptible to higher earthquake ground motions, followed by further integration of available data, such as movements along active faults, focal planes, shear wave velocities, uplift / subsidence estimates, 3D structure, lithologic properties, thickness of lithologic units, etc.

The analysis method and the integration rules can easily be modified in the open GIS architecture as soon as additional information becomes available. The database and maps thus obtained can facilitate and support the planning of additional geotechnical investigations. The more geotechnical site data exists, the better and more detailed the resulting susceptibility maps will be.

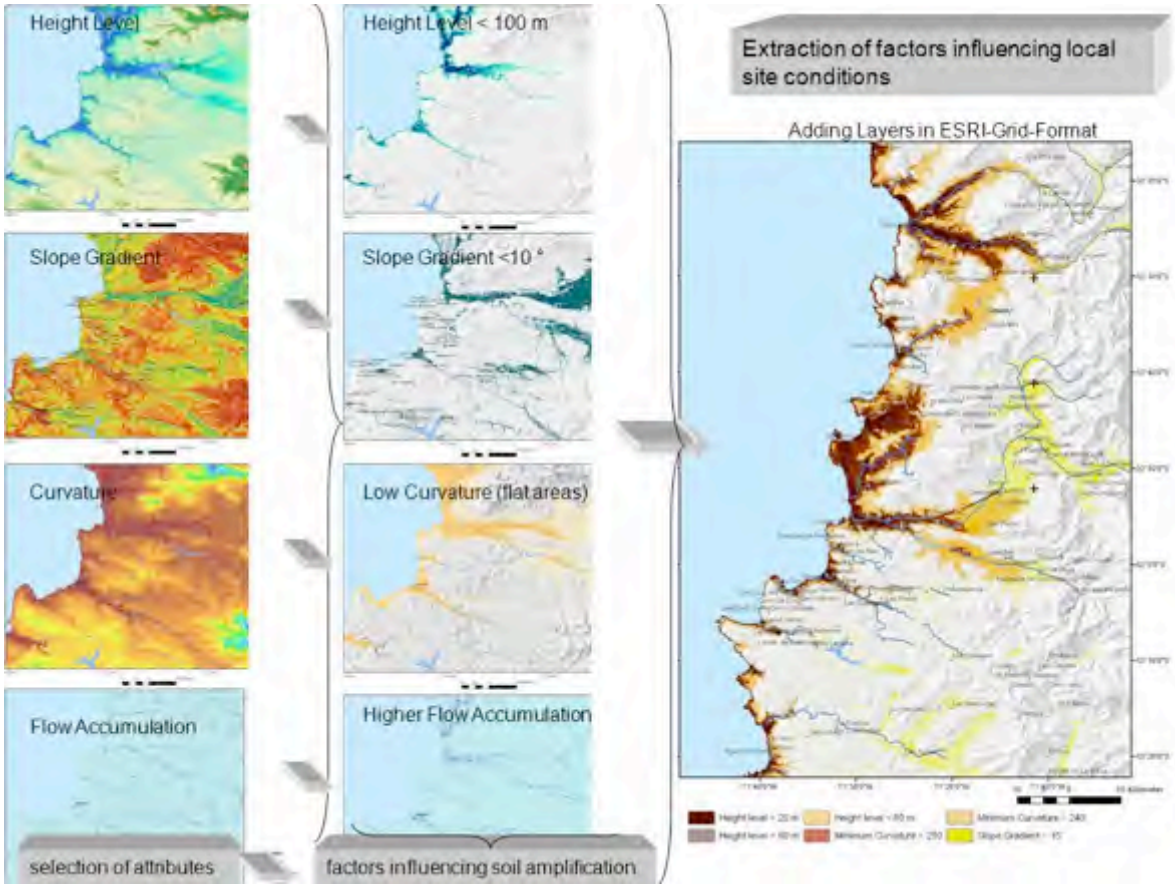

Fig. 3. Basic GIS approach for the extraction of causal factors influencing earthquake shock

3.2. Evaluations of LANDSAT Data

LANDSAT data were processed using various digital image processing methods using ENVI-Software / ITT. The main purpose of this image processing was to enhance the evaluation feasibilities for the detection of local site conditions and for structural analysis by integrating remote sensing and GIS technologies.

3.2.1. Lineament Analysis

Special attention was focussed on precise mapping of traces of faults (lineament analysis) on satellite imageries, predominantly on areas with distinct expressed lineaments, as well as on areas with intersecting/overlapping lineaments. Lineament analysis based on satellite imageries or DEM derived

morphometric maps can help delineate local surface-near fracture systems and faults that might influence seismic wave propagation and influence the intensity of seismic shock or might influence the susceptibility to secondary effects. Areas with intersecting, larger lineaments are probably exposed to relatively higher earthquake shock in case of stronger earthquakes. Linear arrangements of pixels depicting the same color/gray tone were mapped as linear features (the term lineament is a neutral term for all linear, rectilinear or slightly bended image elements). Lineaments often represent the surface expression of faults, fractures or lithologic discontinuities (Fig.4). Lineaments are expressed as scarps, linear valleys, narrow depressions, linear zones of abundant watering, drainage networks, peculiar vegetation, landscape and geologic anomalies. The use of such analysis results is based on the assumption that lineament systems in a satellite image are closely connected and respond to deformation scheme change which is caused by changes of the stress field in the earth's crust. Lineament analysis based on remote sensing data can contribute to the kinematic analysis of the investigation area as the distribution, orientation and density of lineaments constrain the orientation and relative magnitude of principal stress and help examine the geometry of deformation. Often however, the lineament pattern reflects overprinting of complex stress orientation representing changes in the orientation of principal stress over space and time. Lineament analysis can contribute to the detection of structural features that in the field might not be visible or can be mapped only based on time and cost-intensive field investigations.

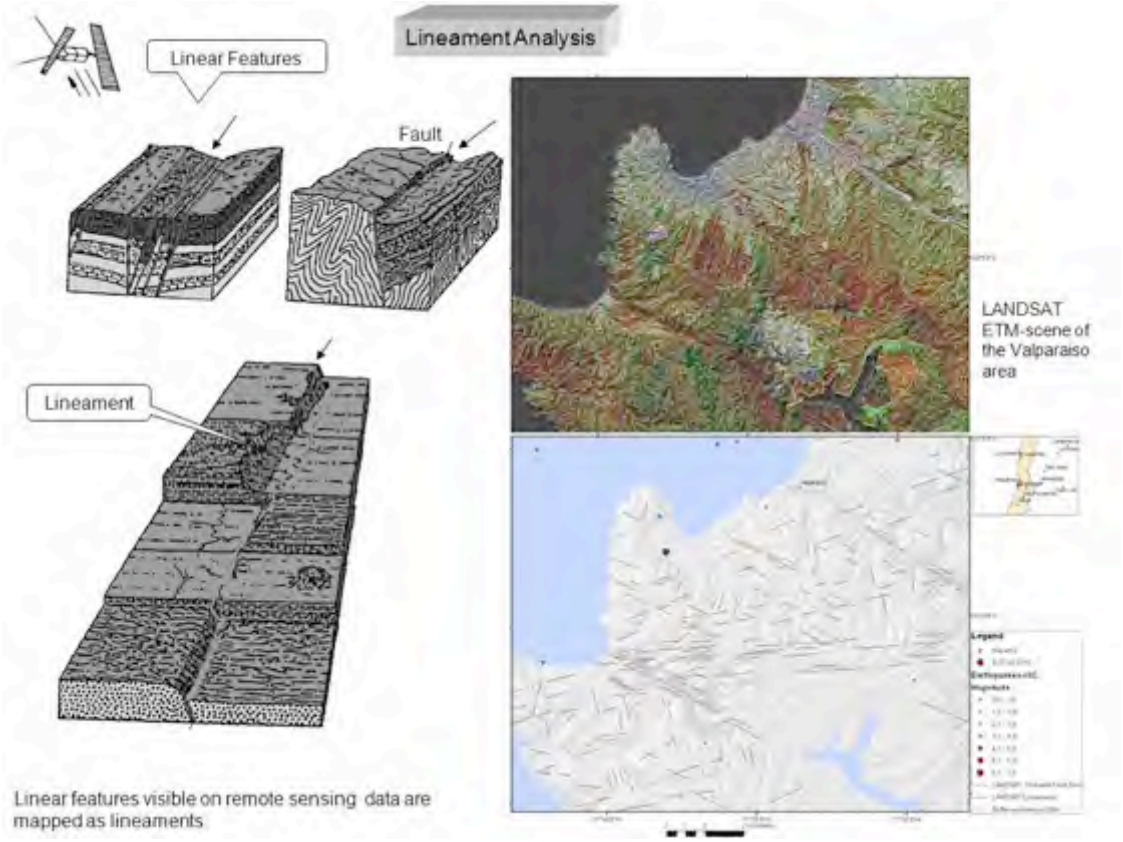

Fig. 4: Lineament analysis based on LANDSAT imageries

3.2.2. Deriving the Water Index (Normalized Difference Water Index – NDWI)

Groundwater table data are an important input when dealing with the seasonal influences on earthquake effects. A promising approach to obtain soil moisture variability is to use the greenness variations of biomass within an otherwise homogeneous canopy, because **variations in soil water directly affect the growth patterns of the overlying vegetation** (DeAlwis et al., 2007). For this purpose vegetation index (NDVI) and water index (NDWI) calculations were carried out (Fig. 5).
By considering information from both the LANDSAT 7 ETM+ Bands 4 and 5 an estimate of the soil moisture setting can be obtained. The Normalized Difference Water Index, NDWI, has been proposed to exploit this characteristic of Bands 4 and 5. The NDWI based on LANDSAT 7 ETM+ Bands 4 and 5 is defined as follows:

$$NDWI = \frac{(780-900\ nm) - (1550-1750)}{(780-900\ nm) + (155-1750)}$$

where (780−900 nm) is the reflectance in Band 4 of LANDSAT 7 ETM+ and (1550−1750 nm) is the reflectance in Band 5 of LANDSAT 7 ETM+. Of the seven bands available from the LANDSAT sensor, this methodology utilised two bands (2/5 and 4/5). The selection of these wavelengths maximises the reflectance properties of water.

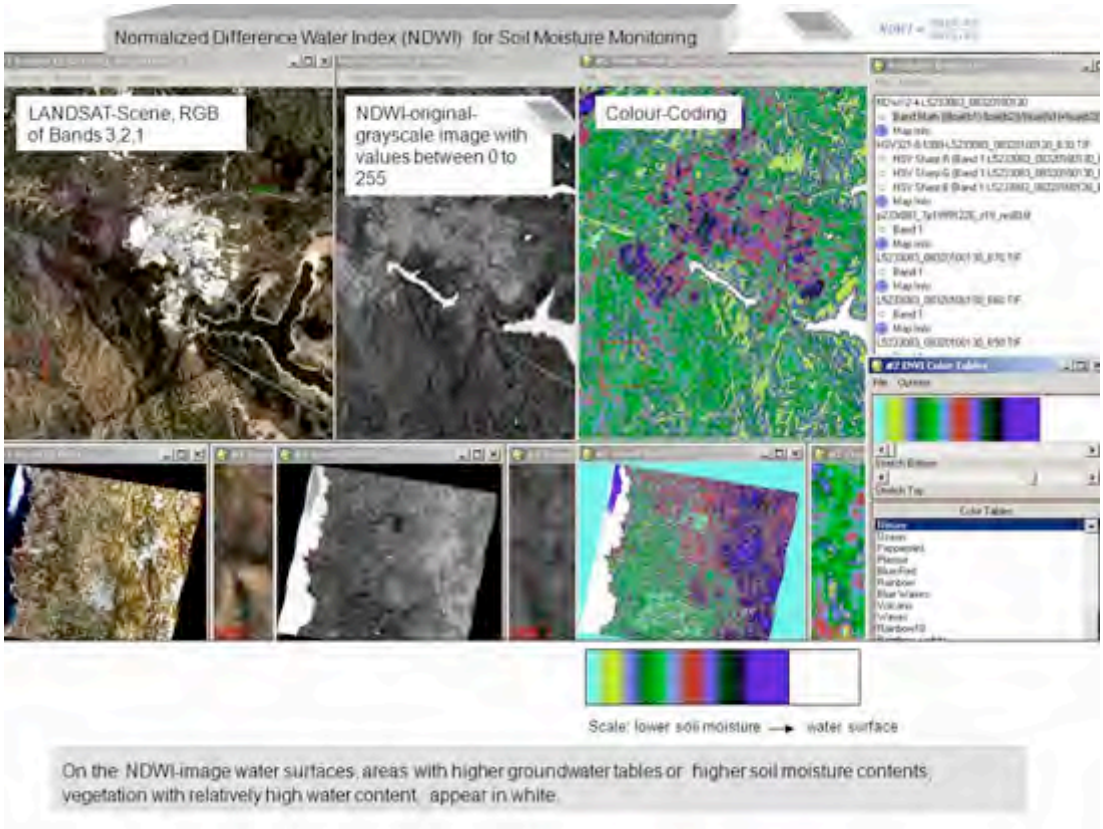

Fig. 5: Water index calculation

After calculating the NDWI in ENVI image processing software an image product with greyscale values between 0 and 255 was created. The NDWI values were ranging from zero to 255 by assigning the least NDWI value in each image cube a value of zero and the maximum NDWI a value of 255. The image products were histogram-stretched and colour-coded and then loaded/integrated into ArcGIS. The result of the histogram stretching was correlated with the visible surface water. In the visible spectrum, reflectance characteristics of surface water can be detected easily. Surface water and water-saturated soils are represented on the chosen colour table in this case in white (Fig. 5). Plants with relatively higher water content appear white as well. Similar spectral response was observed in some cases from larger buildings or shadows in hilly areas. Therefore a careful analysis is necessary.

The patterns in NDWI values for the regions generally represent the temporal variation of surface water size and contour, surface soil moisture (before leaf on) and vegetation water content. The available images were predominantly captured during dryer seasons to minimise cloud cover. This might lead to an underestimation of the true extent of water bodies and to errors. Sensor technical difficulties such as atmospheric haze, poor sensor calibration for some images and, significantly, shadow effects from high topographical areas lead to an overestimation of the water body extent in areas with strong relief. In almost all techniques for mapping water signatures from satellite imagery, shadow areas are a constant noise as the absorption and reflectance of wavelengths in these areas are almost identical spectrally to the absorption and reflectance of wavelengths by large open water features.

As higher values of the NDWI-calculation generally can be correlated with relatively higher water contents at the surface, with higher groundwater tables and surface water, a request was started in ArcMap selecting all values of the NDWI-gray scale image (values:0-255) above 180,…240, and 250), see Fig. 6. These higher values correspond to water surfaces and soils with high water saturation at the acquisition date of the satellite image, what can be confirmed by the visual evaluation of RGB-imageries. This approach, thus, contributes to the detection and the visualization of areas that are more susceptible - in case of a stronger earthquake - to secondary effects such as compaction, liquefaction or soil amplification.

3.2.3. Evaluations of LANDSAT Thermal Bands

An important part of this study was the evaluation of the Thermal Bands 6 of LANDSAT data. All free available, cloud-free LANDSAT data from the USGS and the Global Land Cover Facility of the University of Maryland from 1972 to 2011 were digitally processed. When colour-coding the thermal LANDSAT bands from the coastal area of Valparaiso, water currents at the acquisition time become clearly visible. Of course, these images almost reflect the water, wind and temperature conditions at the data acquisition time. Nevertheless, the streaming pattern visible on the LANDSAT imageries provides some useful information of the influence of coastal morphology on water currents that might be of interest for the better understanding of tsunami wave propagation. These imageries were merged with bathymetric maps of this area in order to investigate whether the sea bottom topography might be traced by the water current pattern at the sea surface (Fig. 7).

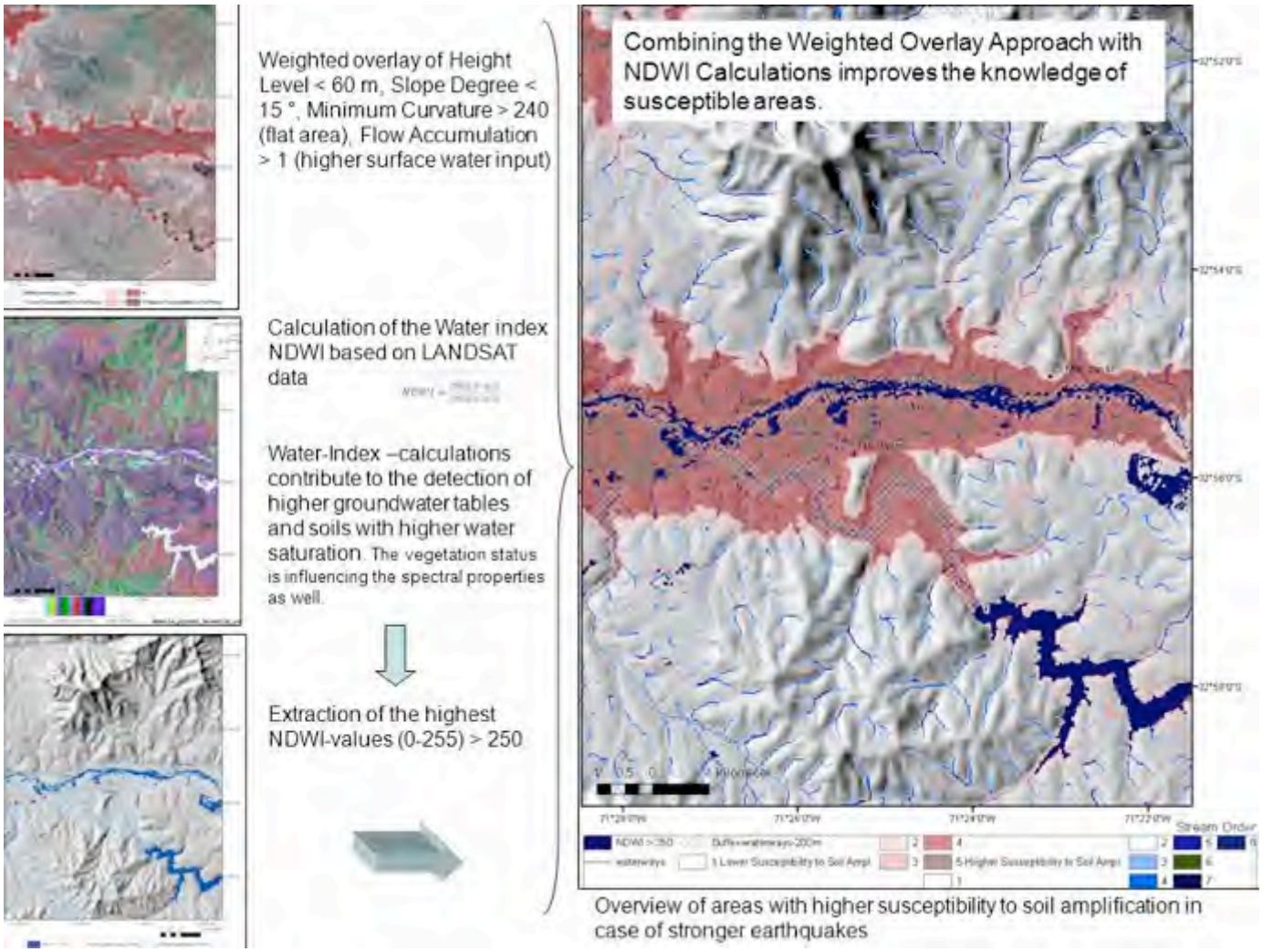

Fig. 6: Normalized Difference Water Index (NDWI) calculation based on LANDSAT TM data and extraction of highest value

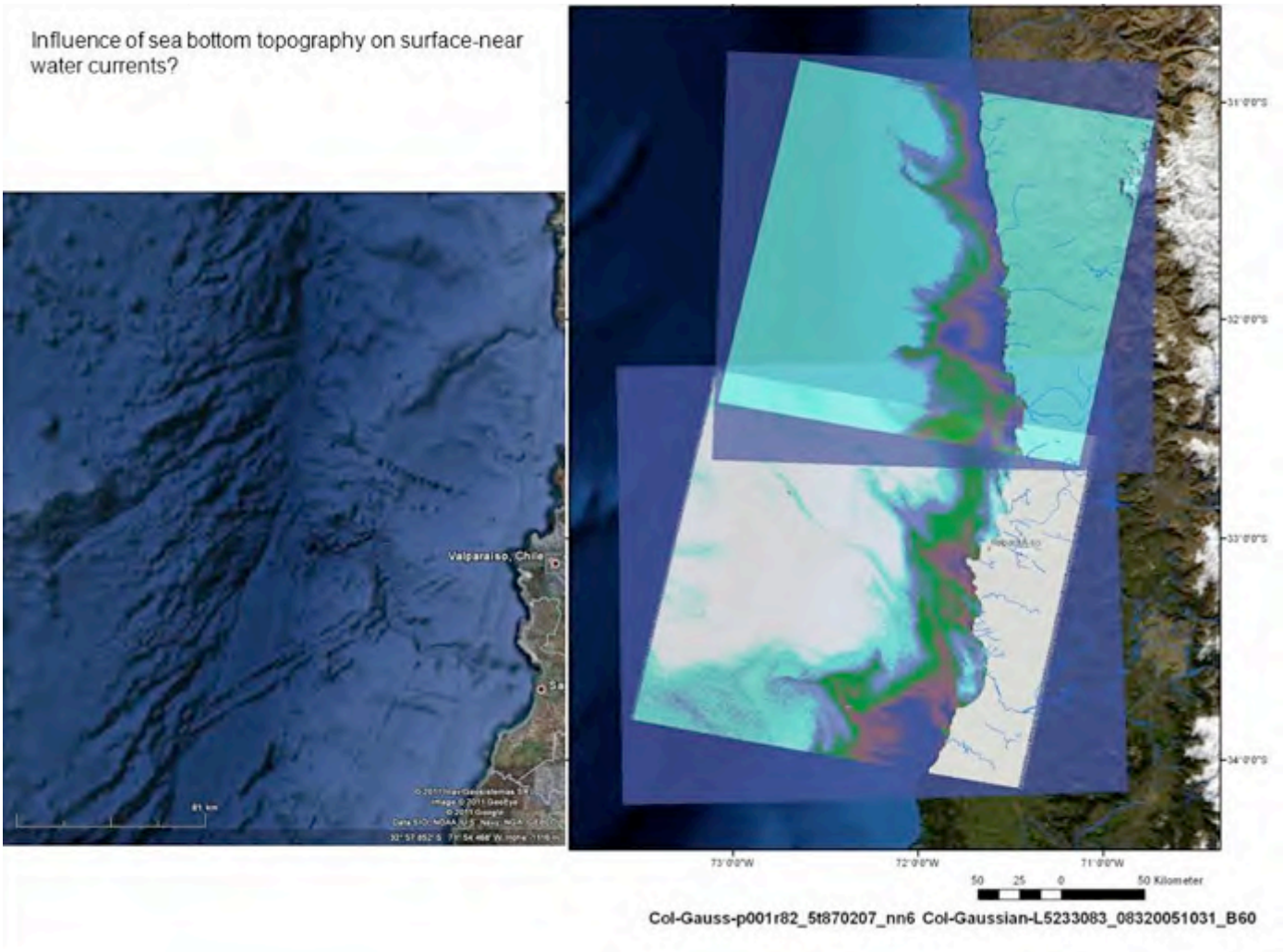

Fig. 7: Colour-coding the Thermal Bands 6 of the LANDSAT satellite data in ENVI software

4. RESULTS OF THE GIS INTEGRATED EVALUATIONS OF REMOTE SENSING DATA

4.1. Results of the Weighted Overlay Methods

After evaluating the ASTER and SRTM DEM data, gaining morphometric maps, extracting causal factors with influence on local site conditions as shown in Fig. 3. Using the weighted overlay tool in ArcGIS, an overview of areas more susceptible to soil amplification in case of stronger earthquakes can be obtained. Comparing these results with geologic maps, it can be stated that these areas correspond to outcrops of unconsolidated, Quaternary sediments. The following figures demonstrate these areas in red to dark-red colours (Figs. 8 and 9).

Lineaments mapped based on the LANDSAT images are included into the maps in order to get more information of the structural pattern and its potential influence on seismic wave propagation, and of active shear zones with movements.

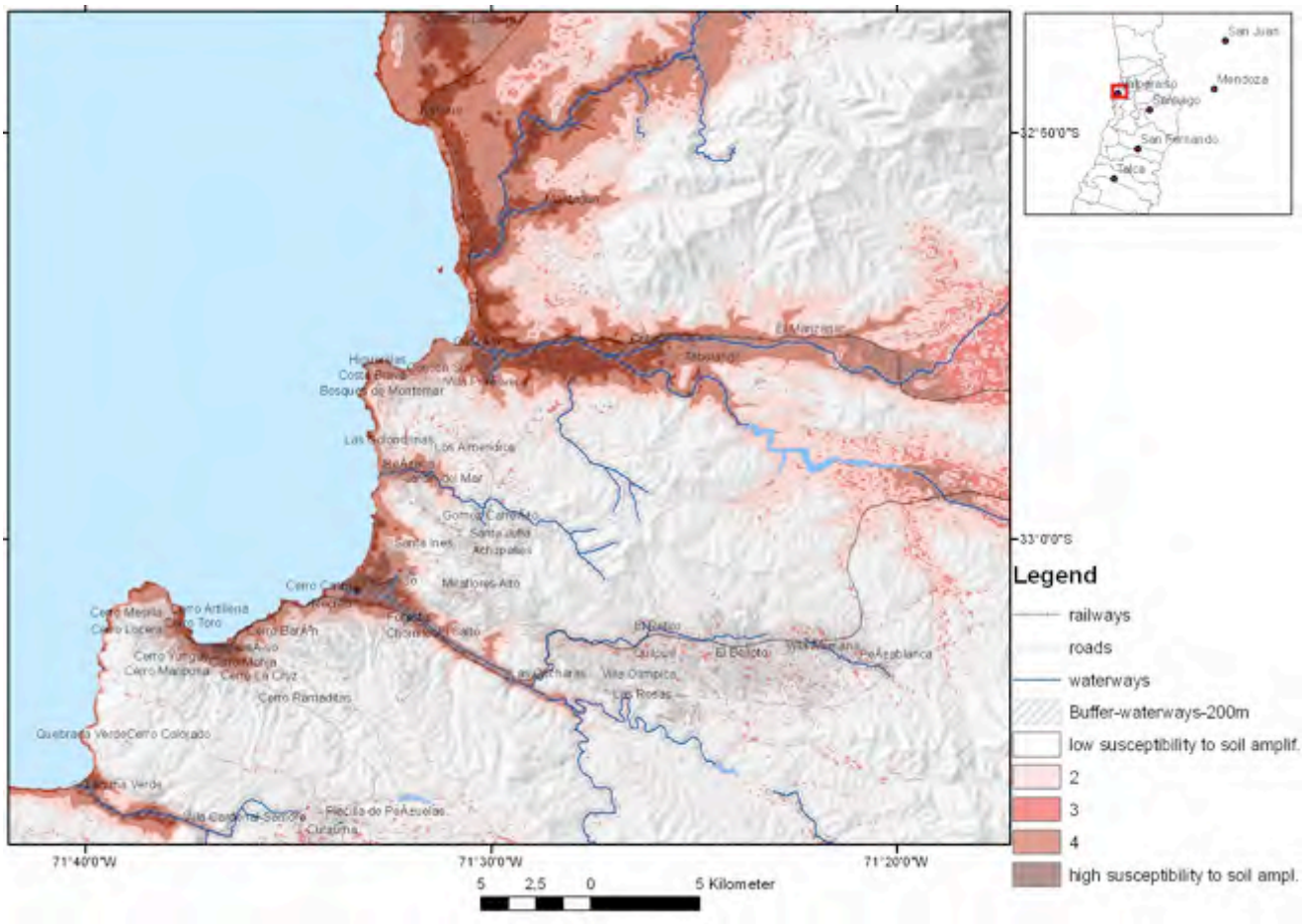

Fig. 8: Susceptibility to soil amplification according to the weighted-overlay-method based on ASTER DEM data

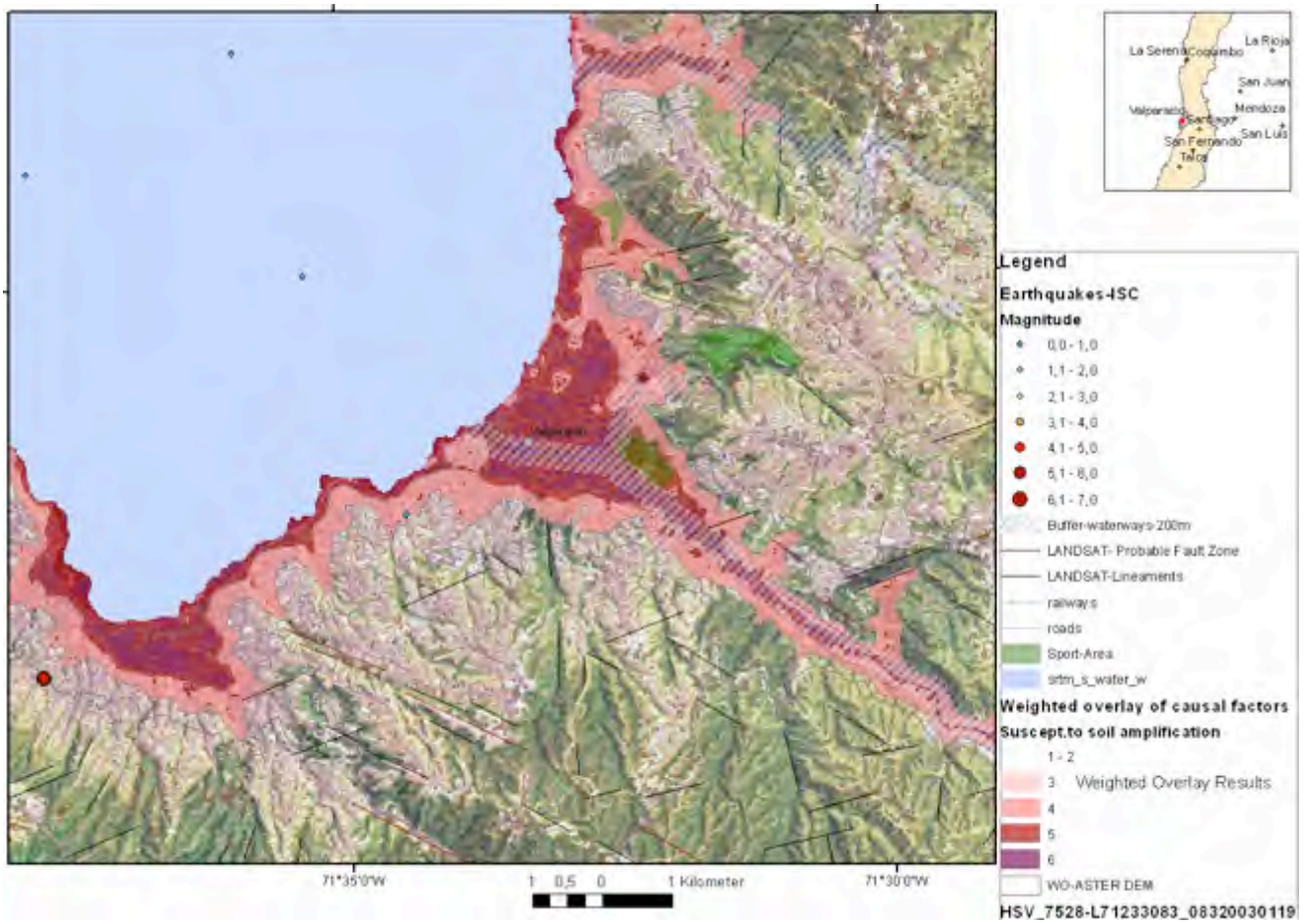

Fig 9: Susceptibility to soil amplification according to the weighted-overlay-method based on ASTER DEM, LANDSAT data, geologic maps and earthquake data

Aggregating following factors: [height level < 10m] + [slope degree < 10°] + [curvature = 0] + [flow accumulation >1] + [outcrop of Quaternary sediments-Grid] + [fault zones-Grid] Dark-red areas correspond to the areas where nearly all "causal" factors overlap.

ShakeMaps showing the distribution of recorded peak ground acceleration (PGA) and peak ground velocity (PGV) overlain on regional topography maps allow to gauge the effects of local site amplification because topography is a simple proxy for rock versus deep-basin soil-site conditions. This can lead to more detailed investigations into the nature of the controlling factors. Peak velocity values are contoured for the maximum horizontal velocity (in cm/sec) at each station. (PGA is peak ground acceleration in units of %g, PGV is peak ground velocity in units of cm/s). Typically, for moderate to large events, the pattern of peak ground velocity reflects the pattern of the earthquake faulting geometry, with largest amplitudes in the near-source region, and in the direction of rupture (directivity). Differences between rock and soil sites become apparent (USGS, access: 2011).

The following figure shows an overlay of shake maps from larger earthquakes with the weighted overlay results (Fig.10). The combination of these two approaches allows a better overview of areas probably prone to higher earthquake shock due to local site conditions within one calculated shake zone.

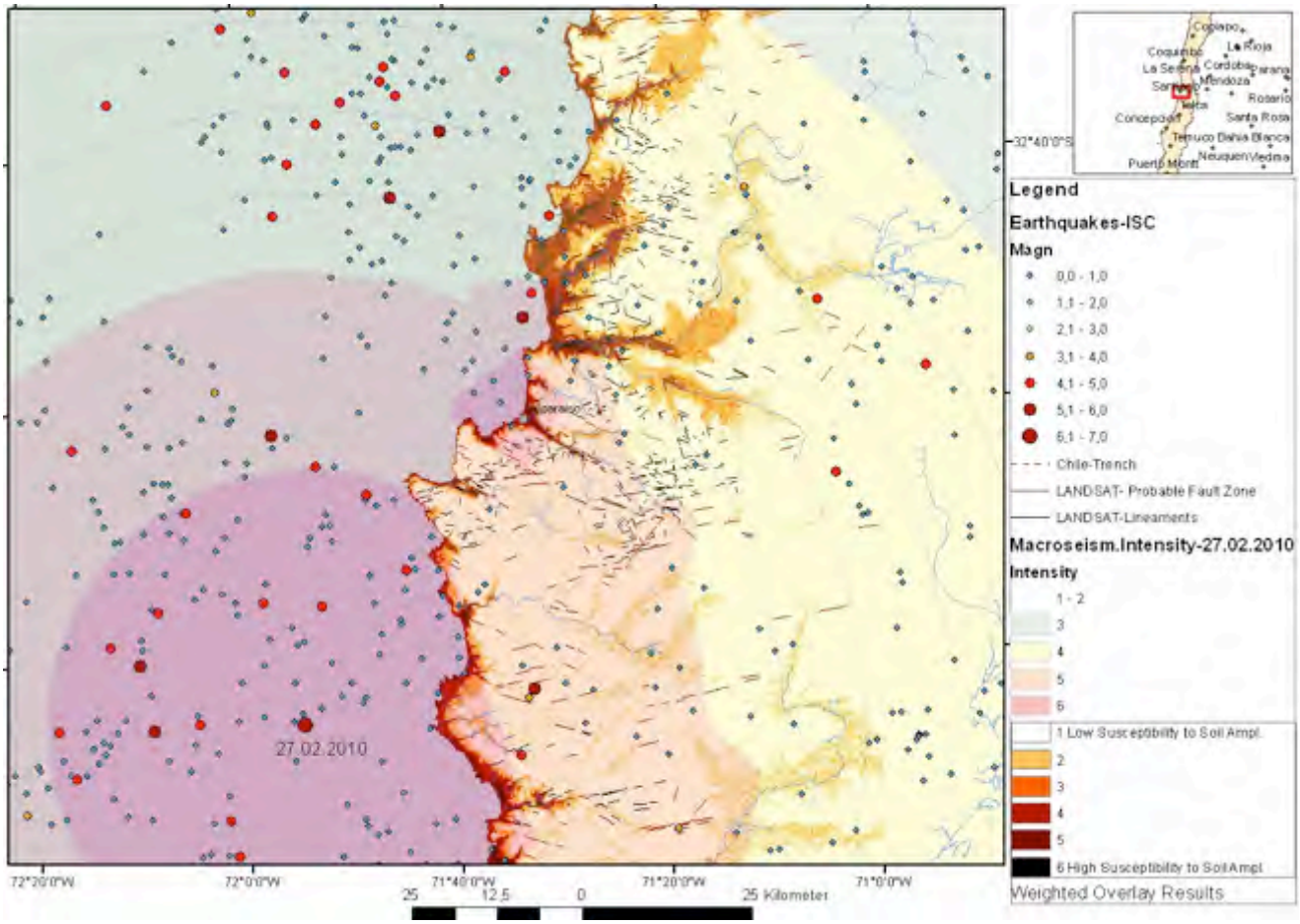

.

Fig. 10: Overlay of the macroseismic intensity-map (shakemap according to USGS) with the results of the weighted overlay calculations of morphometric factors influencing local site conditions based on ASTER DEM data

4.2. Evaluation Results based on LANDSAT image data

The structural evaluation of the LANDSAT images allows the detection of linear features due to their morphologic expression and/or linear tone anomalies. Using the filter tools in ENVI the detection of the lineaments was improved. Fig. 11 shows the results of the water index calculations based on LANDSAT data of different years and seasons. The varying water content in the plants and soils becomes clearly visible.

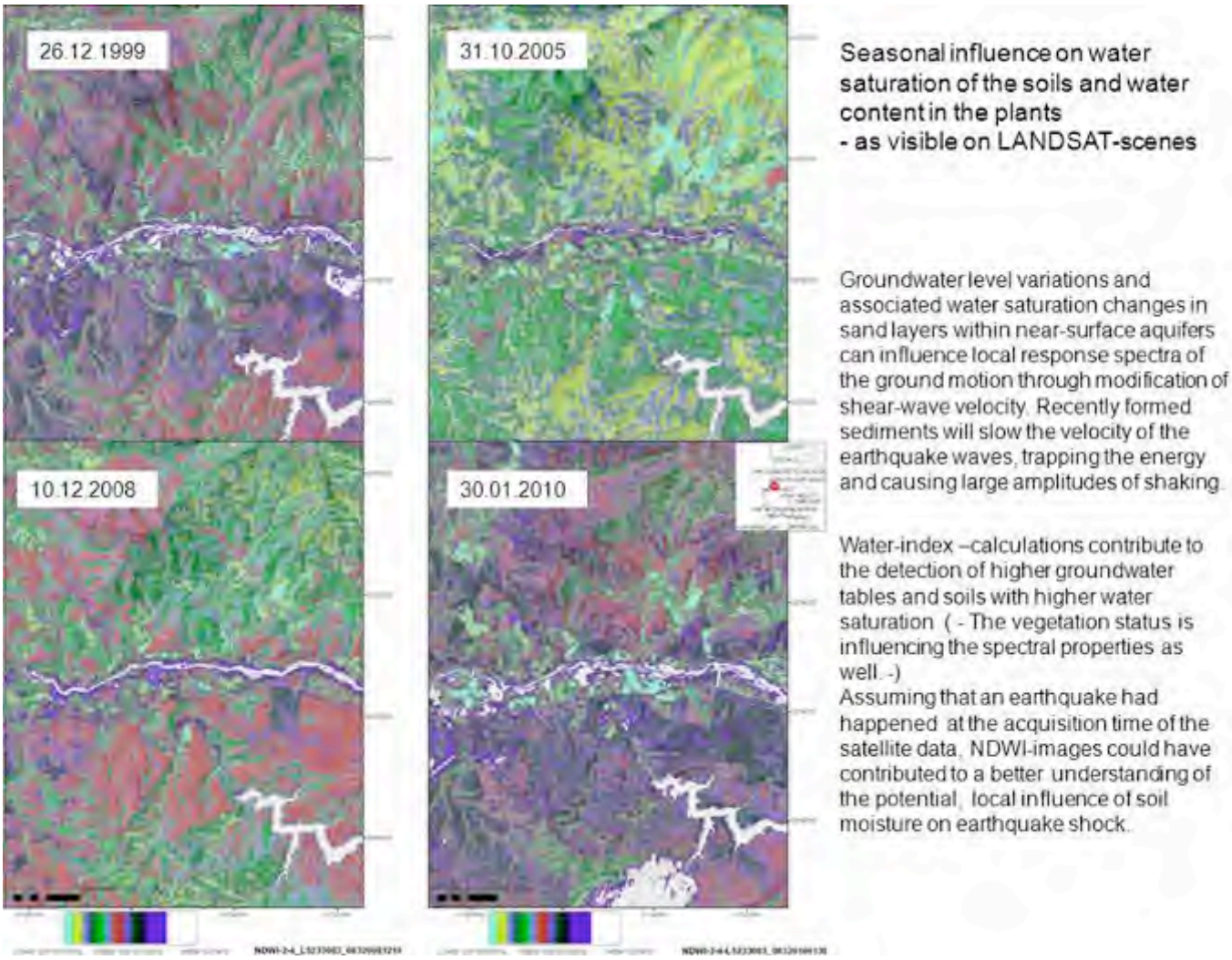

Fig. 11: NDWI calculations based on LANDSAT imageries of different seasons and years for visualizing seasonal variations.

The highest NDWI values were extracted and merged with the weighted overlay results (Fig. 12). Whenever a stronger earthquake occurs, NDWI calculations based on at the same time available image data like RapidEye or Sentinel data can quickly provide an overview of the soil moisture conditions that might have an influence on earthquake shock intensity.

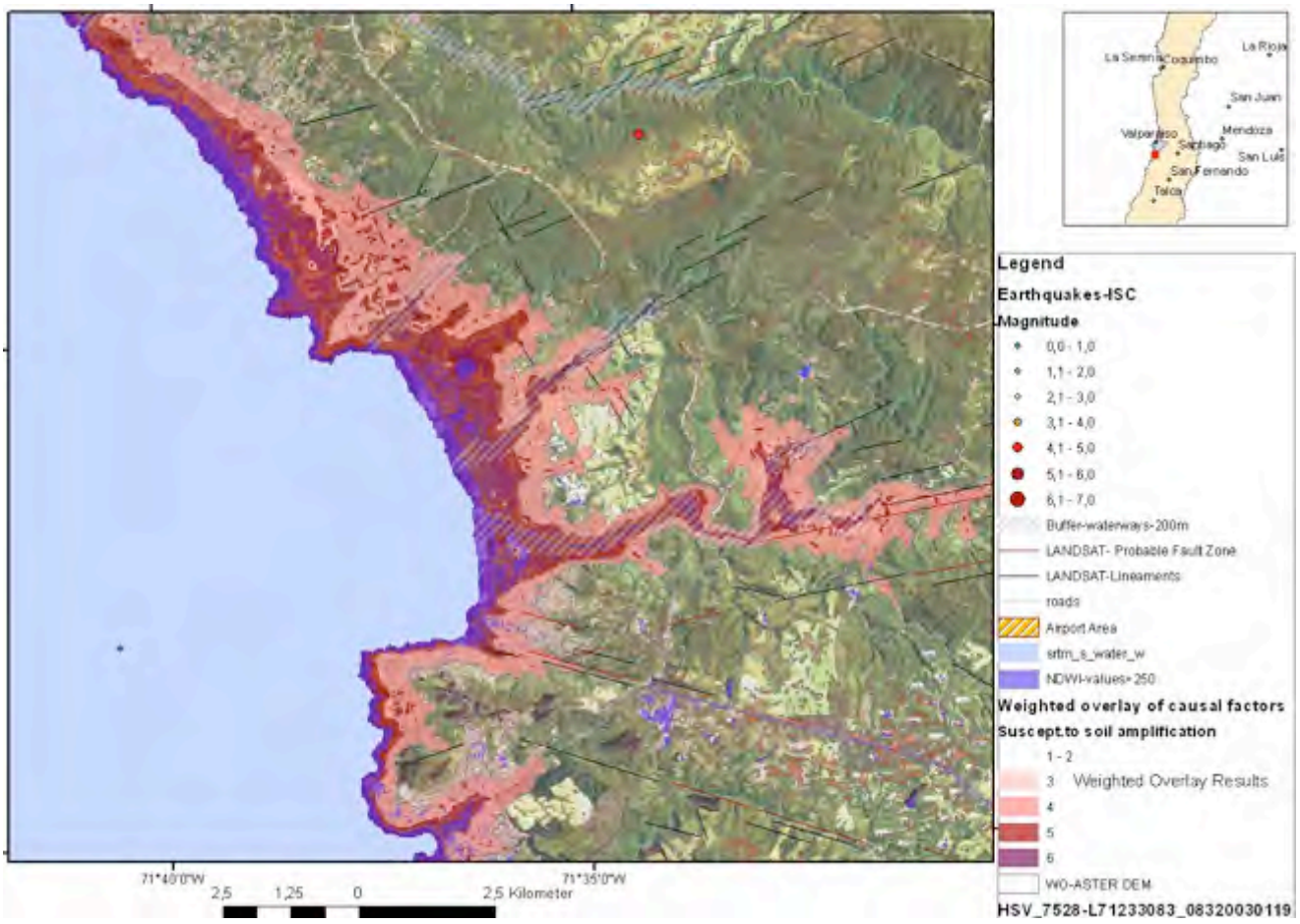

Fig.12: Extraction of the highest NDWI-values (lila) based on different LANDSAT data for visualizing potential influences of soil moisture on earthquake shock intensity

5. SHEAR WAVE VELOCITIES

Shear-wave velocity is an important factor when investigating local soil conditions. A standardized approach for mapping seismic site conditions measuring or mapping shear-wave velocity (*V*S) was developed by Wald & Allen (2007). As in many seismically active regions of the world, information about surficial geology and *V*S either, does not exist, varies dramatically in quality, varies spatially, or is not easily accessible Wald & Allen first correlated *V*S 30 (here V_S^{30} refers to the average shear-velocity down to 30 m) with topographic slope (m/m) at each *V*S 30 measurement point for data. The basic premise of the method is that the topographic slope can be used as a reliable proxy for V_{S30} in the absence of geological and geotechnical based site-condition maps through correlations between V_{S30} measurements and topographic gradient. By taking the gradient of the topography and choosing ranges of slope that maximize the correlation with shallow shear-velocity observations, it is possible to

recover, to first order, many of the spatially varying features of site-condition maps. It is worth noting that the resolution (30 arc sec) of the topography allows relatively detailed maps of site conditions. Many of these details come from small-scale topographic features that are likely to be manifestations of real site differences, such as basin edges and hills protruding into basins and valleys - and are thus easily visible due to their significant slope change signatures. Typically, these edges are important for predicting ground motion variations due to earthquakes (Wald and Allen, 2007). Thus, from the Valparaiso area the derived Vs (m/sec) data were downloaded from the USGS and integrated and interpolated in ArcGIS for getting an overview of the estimated shear velocities in case of larger earthquakes (Fig. 13). Lower shear wave velocities up to 400 m/s as derived by Wald & Allen correspond quite well with the outcrop of unconsolidated, Quaternary sediments in the broader valleys. Merging the Weighted-Overlay-Susceptibility map with the Vs-data derived by Wald and Allen (2007) there is a coincidence of areas assumed to be more susceptible to soil amplification according to the weighted overlay approach with areas of estimated lower shear wave velocities (Vs < 250, Fig.14).

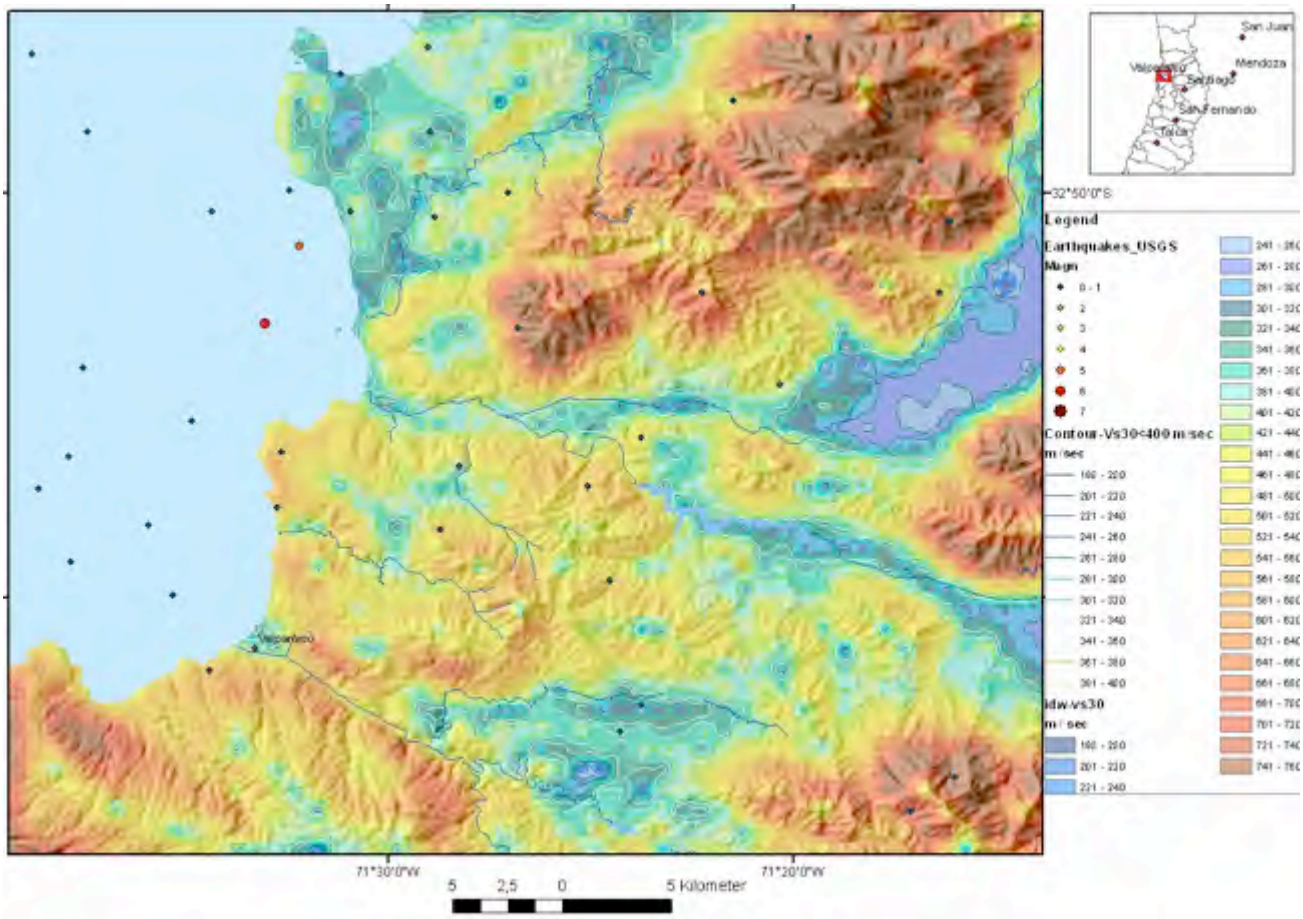

Fig. 13: Estimated shear wave velocities (Vs) in the Valparaiso-area area as derived by Wald and Allen (2007)

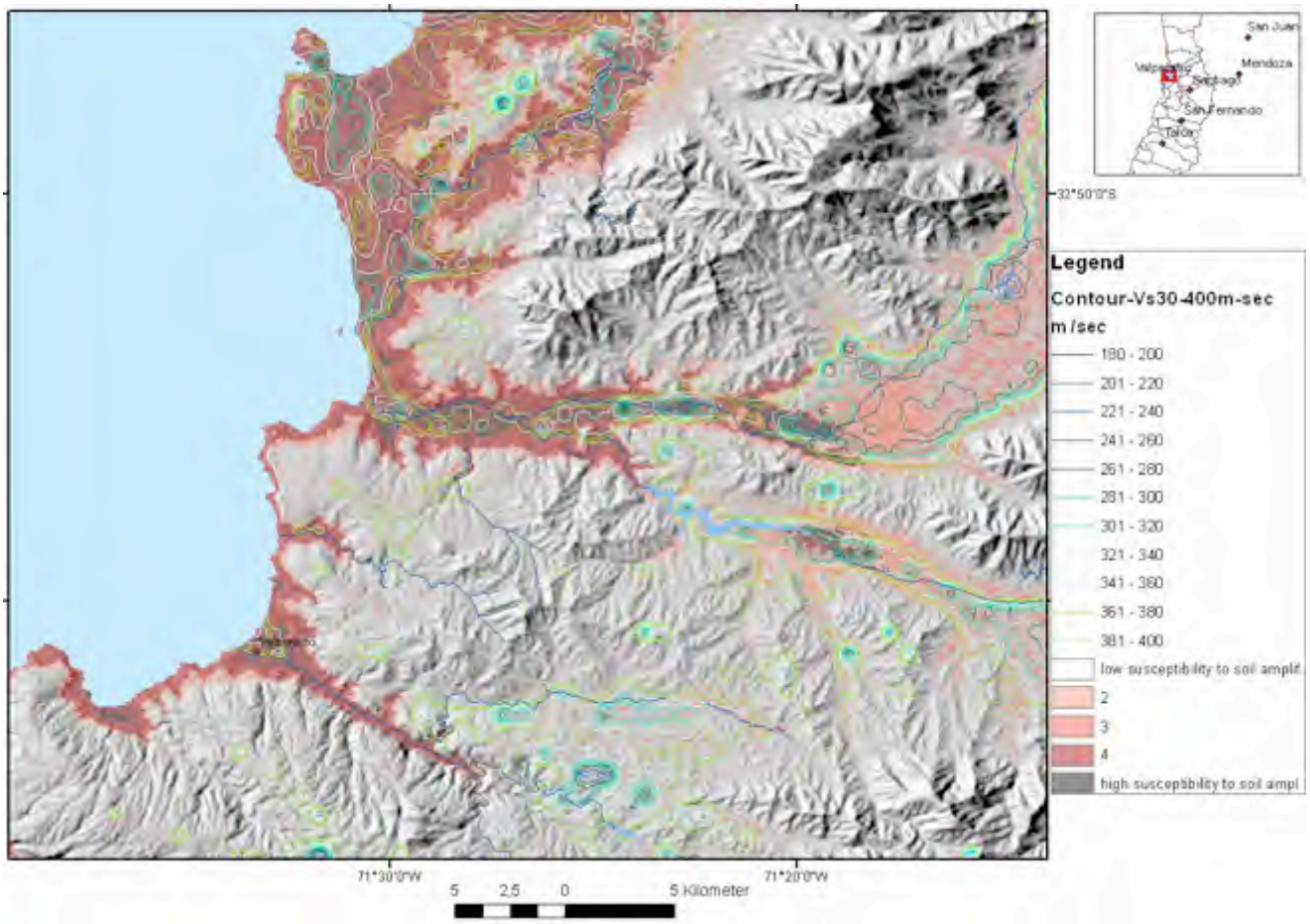

Fig.14: Merging assumed shear velocity data (Vs30 < 400 m/sec) from USGS as contour lines with the soil amplification susceptibility map according to the weighted overlay-approach.

6. FLOODING SUSCEPTIBILITY

The Chilean coast is currently exposed to the effects of near and far field tsunamis generated in the Pacific Ocean (Gutierrez, 2005). Tsunami waves have been documented after various larger earthquakes (Figs. 1 and 15). For instance, the catastrophic events of the last century, in 1868 and 1877, overwhelmed the coast of the northern region of the country. In the younger history there are 6 earthquakes related with the occurrence of tsunami waves in the Bay of Valparaiso: 13.05.1647, 08.07.1730, 19.11.1822, 16.08.1906, 03.03.1985 and 27.02.2010 (Pararas-Carayannis, 2010). During this century, the most important disaster was the 1960 earthquake and tsunami in Valdivia. An overview of tsunami events in Chile is provided by NOAA's Satellite and Information Service (NESDIS) and by the Servicio Hidrografico y Oceanografico de la Armada de Chile.

The planning of economic activity and any new constructions in these seismically active and tsunami risk zones of the Chilean coast requires preliminary estimates of the possible flooding extent related to tsunamis. Most tsunamis are generated by submarine earthquakes, also by inland /coastal earthquakes, turbidity currents and landslides. Tsunami propagation is sensitive to sea bathymetry. Tsunami impact on the coast and flooding is influenced by coastal topography. Ridges rising from the ocean floor such as seamounts/guyots, or deeper canyons, may have an influence of the tsunami energy propagation. In case of storm floods or stronger tsunami events the coastal morphology and islands will modify the flooding dynamics. The interaction of tsunami waves with local elements is governed by the geometrical scale of the obstacles.

Based on the aforementioned geospatial data sets, a number of tsunami hazard-controlling parameters are derived, including elevation, slope, aspect, curvature, concavity, soil types, land use classification, and hydrological variables (drainage density, flow accumulation and flow path). By using GIS-based map overlay techniques, the derived tsunami susceptibility values are the weighted linear summation of the controlling or causal factors such as slope, curvature, flow accumulation, soil type, soil texture, elevation, vegetation cover and drainage pattern.

Summarizing factors influencing flooding susceptibility such as relatively lowest height levels (< 10 m), minimum terrain curvature (values=0), slope gradients below 10° and high flow accumulation values using the weighted-overlay tools in ArcGIS helps to map areas susceptible to flooding, see Fig. 15. As river mouths form an entrance for flooding waves, those areas along the river sides are even more susceptible to flooding, visualized in the GIS by a 100 m and 200 m-buffer-layer along the waterways.

The evaluation of LANDSAT imageries can contribute to a better understanding of surface-near water streaming mechanisms. When colour coding and classifying LANDSAT imageries of different acquisition dates water currents become visible (Figs. 16 to 18). The colour-coded thermal imageries provide an overview of the different streaming pattern during the image acquisition. Merging the thermal imageries with the bathymetric map, it seems that subsurface structures as canyons and terraces influence even the near-surface water streaming (Figs. 19 and 20). Especially above submarine canyons, water currents can be observed. In case of tsunami waves it can be assumed that the coastal morphology could cause similar effects.

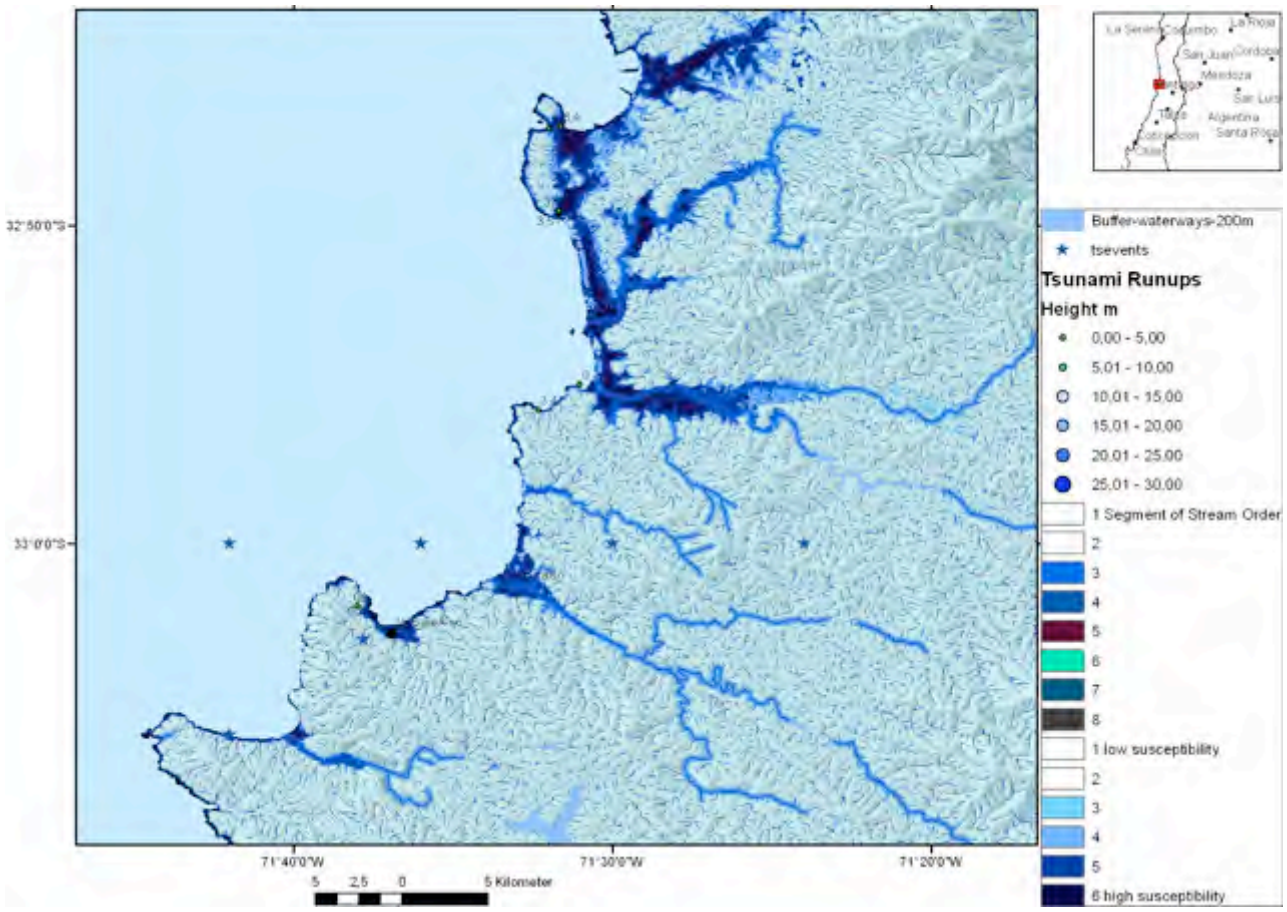

Fig. 15: Flooding susceptibility map of Valparaiso in case of storm surges, flash floods or tsunami waves based on the aggregation of the following factors (based on SRTM DEM) using the weighted overlay-tool of ArcGIS: [height level <5- 10 m] + [slope degree < 10°]+[curvature=0]+ [high flow accumulation]+ river mouths and estuaries-Grids, Buffer of 200 m along the waterways.

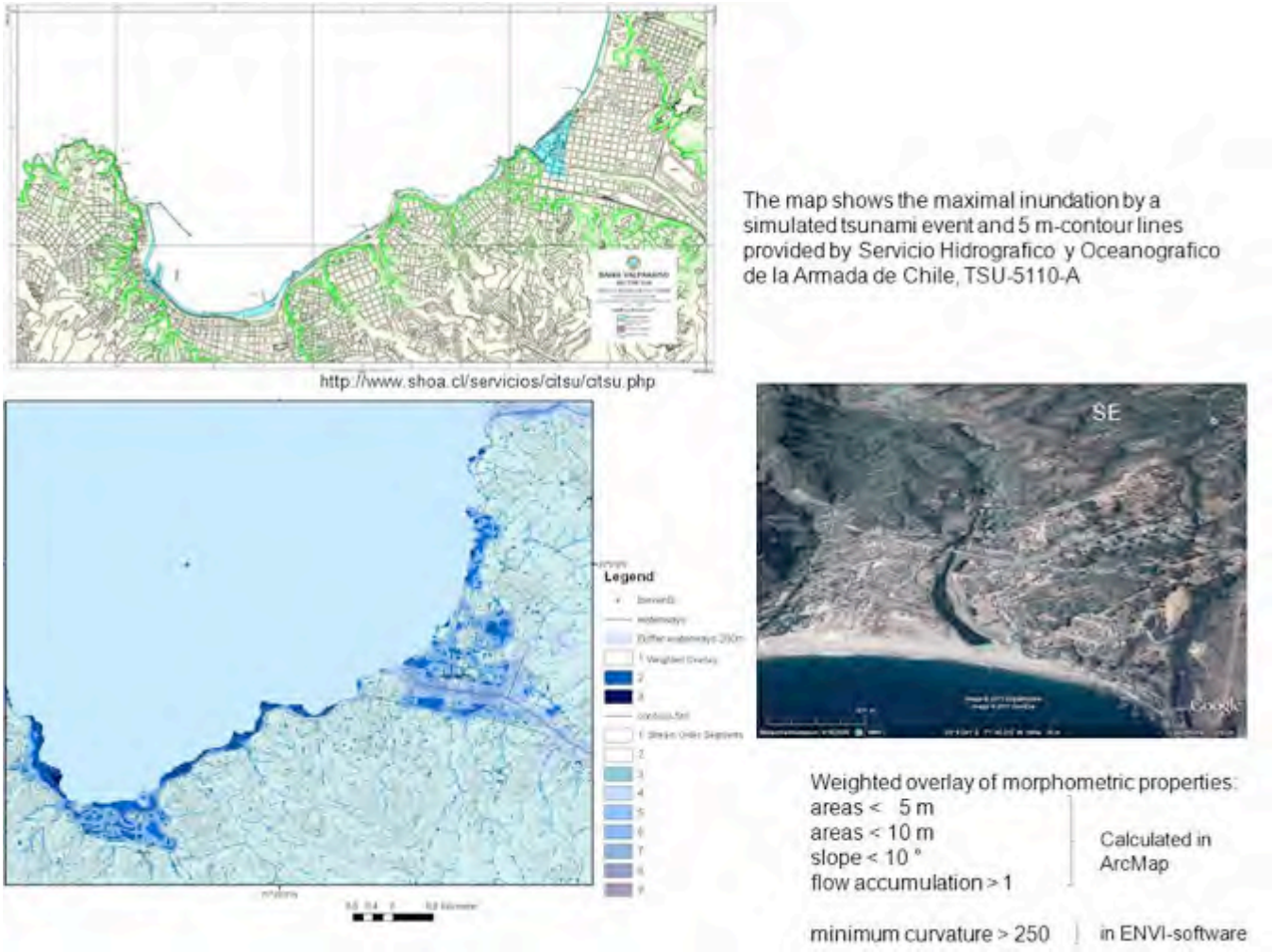

Fig. 16. Comparison of the weighted overlay results (based on ASTER DEM data) and a simulated tsunami inundation map of Valparaiso

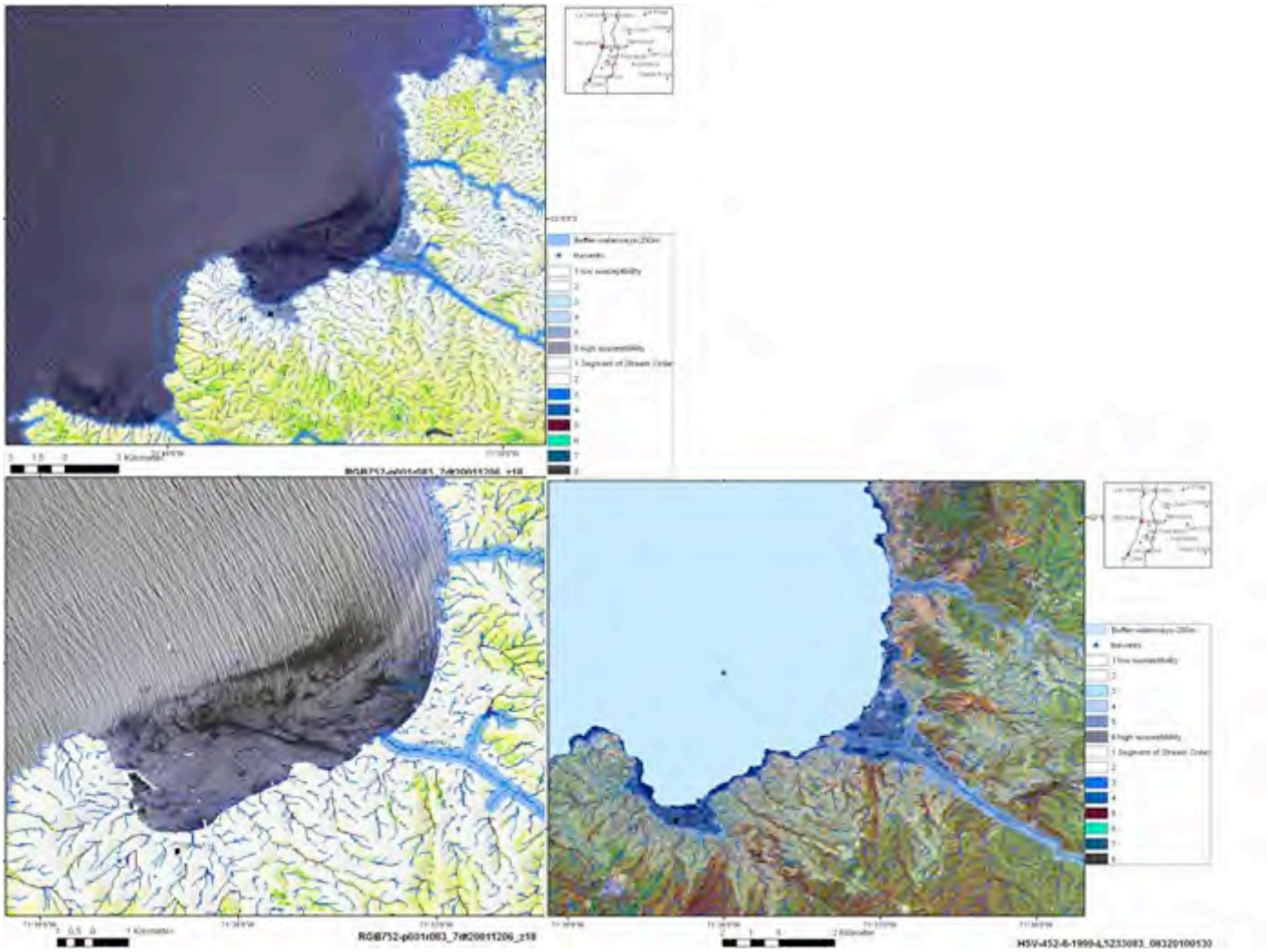

Fig. 17: Wind driven surface waves at the coast of Valparaiso and areas susceptible to tsunami flooding

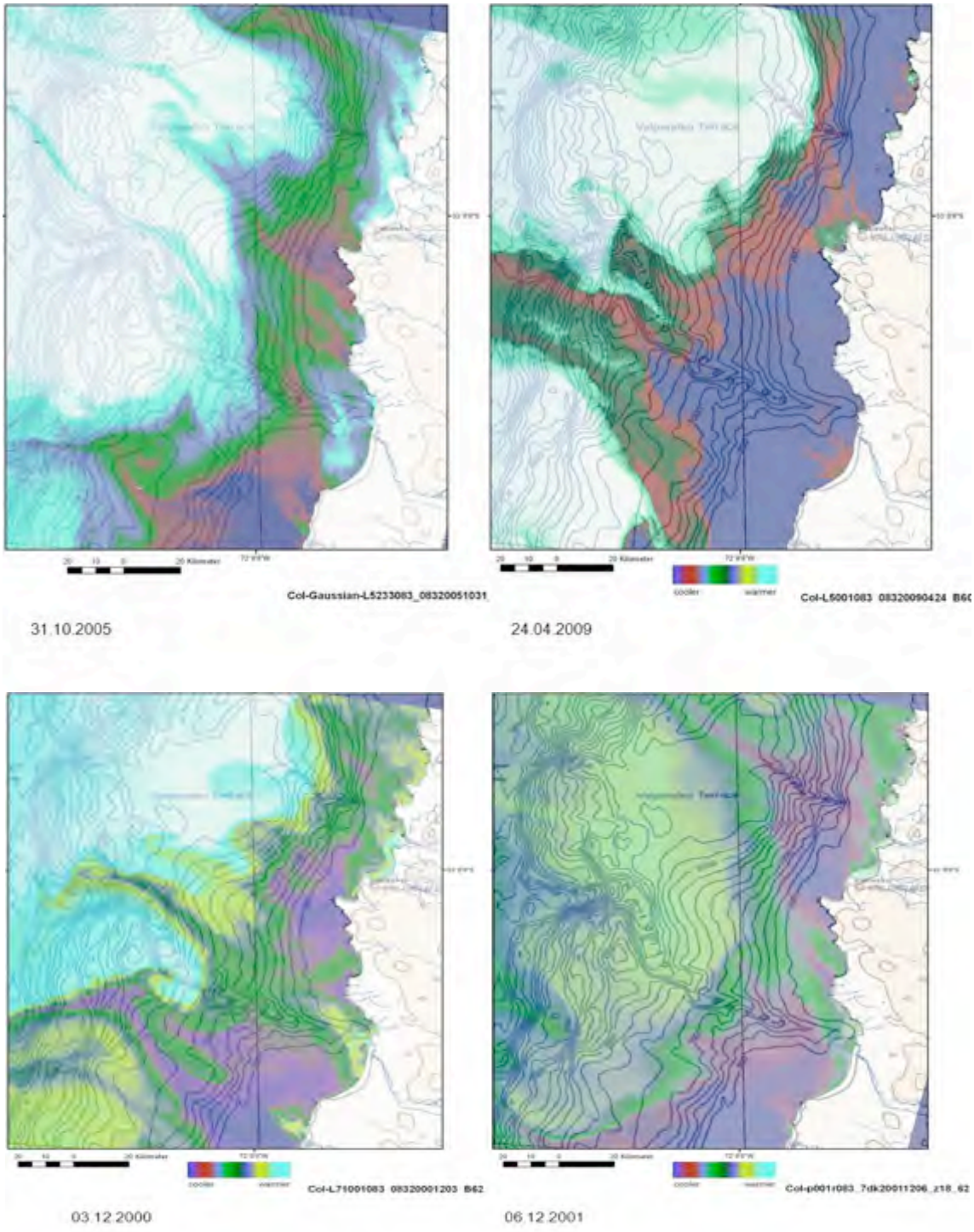

Fig. 18 a, b: Influence of subsurface-topography on surface-near water currents. Comparison of the bathymetric map and colour-coded LANDSAT Band 6-imageries

The concentration of larger fault zones and fault and fracture zones intersecting each other are important factors influencing slope instability onshore and offshore. The almost detailed detection of those larger offshore faults, especially when active, based on geophysical, geodetic and bathymetric data is most important, as these areas might be potential tsunami source regions.

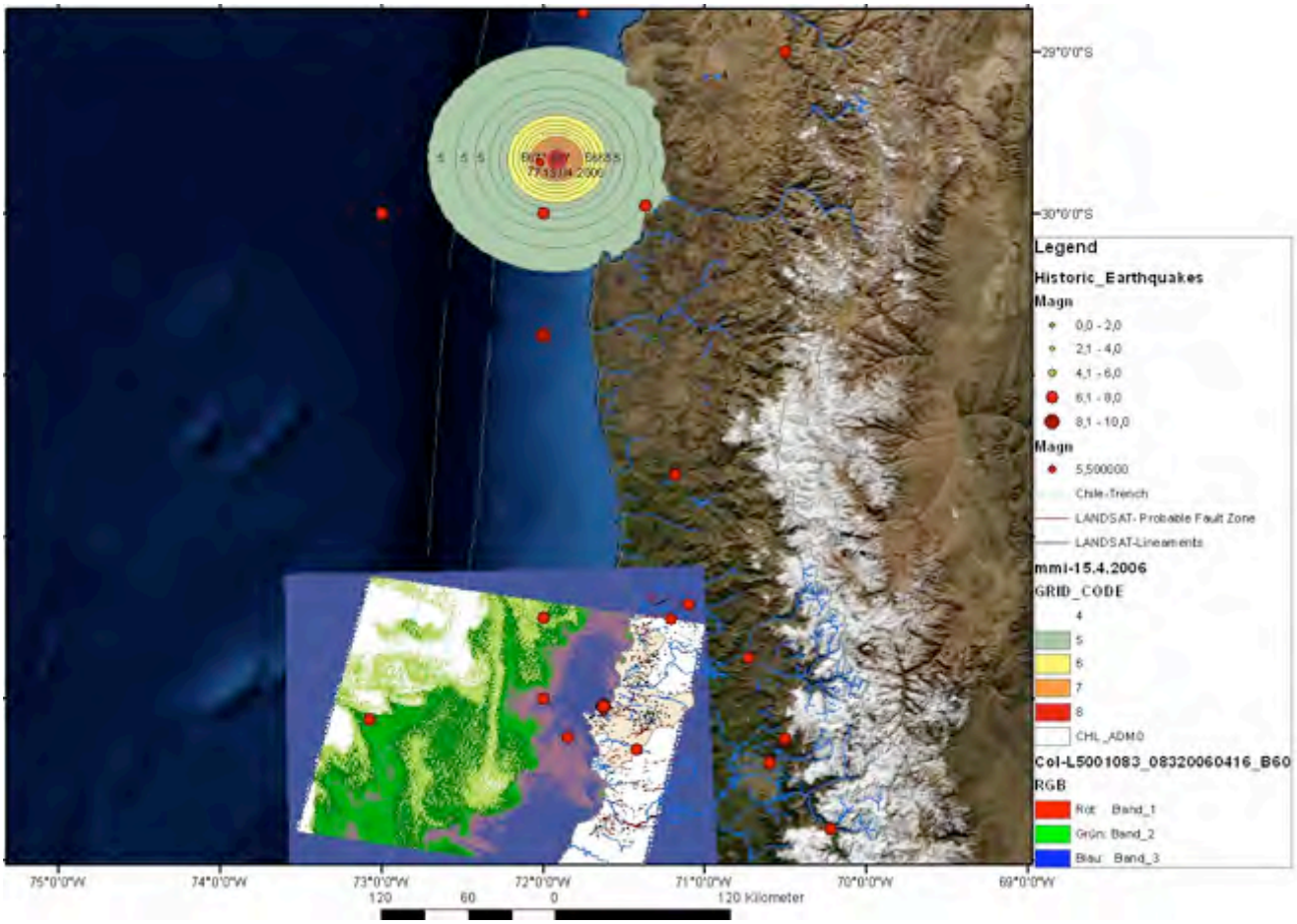

Fig. 19: Earthquake / tsunami (?) induced changes in the surface-near streaming pattern. According to USGS a stronger earthquake (M 6) happened a day before this image was taken.

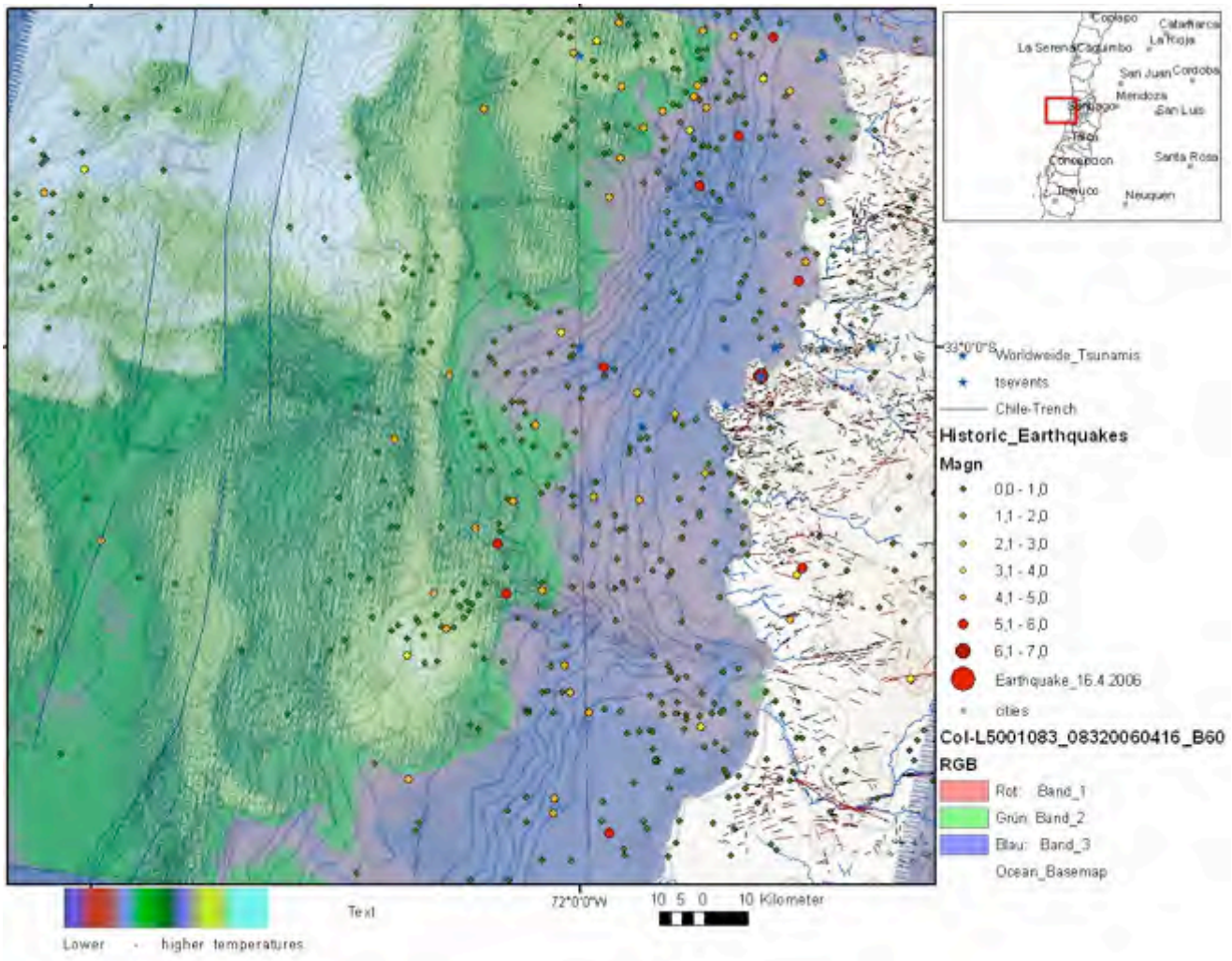

Fig. 20: Sea-surface temperature anomalies on 16.04.2006

7. SUSCEPTIBILITY TO SLOPE FAILURE

After larger earthquakes newly formed landslides were observed (USGS, 1985). The mountainous areas were subjected to landslides after the quake shattered exposed areas, especially those that were prone to previous slope failure in the past. Areas susceptible to slope failure that could be affected by stronger earthquakes should be considered when planning the rebuilt of affected cities. Identification and mapping of instability factors having a relationship with the slope failures require knowledge of the main causes of landslides. These instability factors include lithologic properties of the surface rocks and soil properties, the tectonic pattern, seismicity, slope steepness and curvature, stream evolution, groundwater conditions, climate conditions, vegetation cover and land use.

Figure 21 shows the result of the Weighted-Overlay-aggregation of these main preparatory factors and lineament analysis. Causal or preparatory factors such as steep slopes, convex curvatures, height levels, drainage pattern and lineaments were extracted from recent LANDSAT ETM-, Google Earth- and ASTER- satellite data.

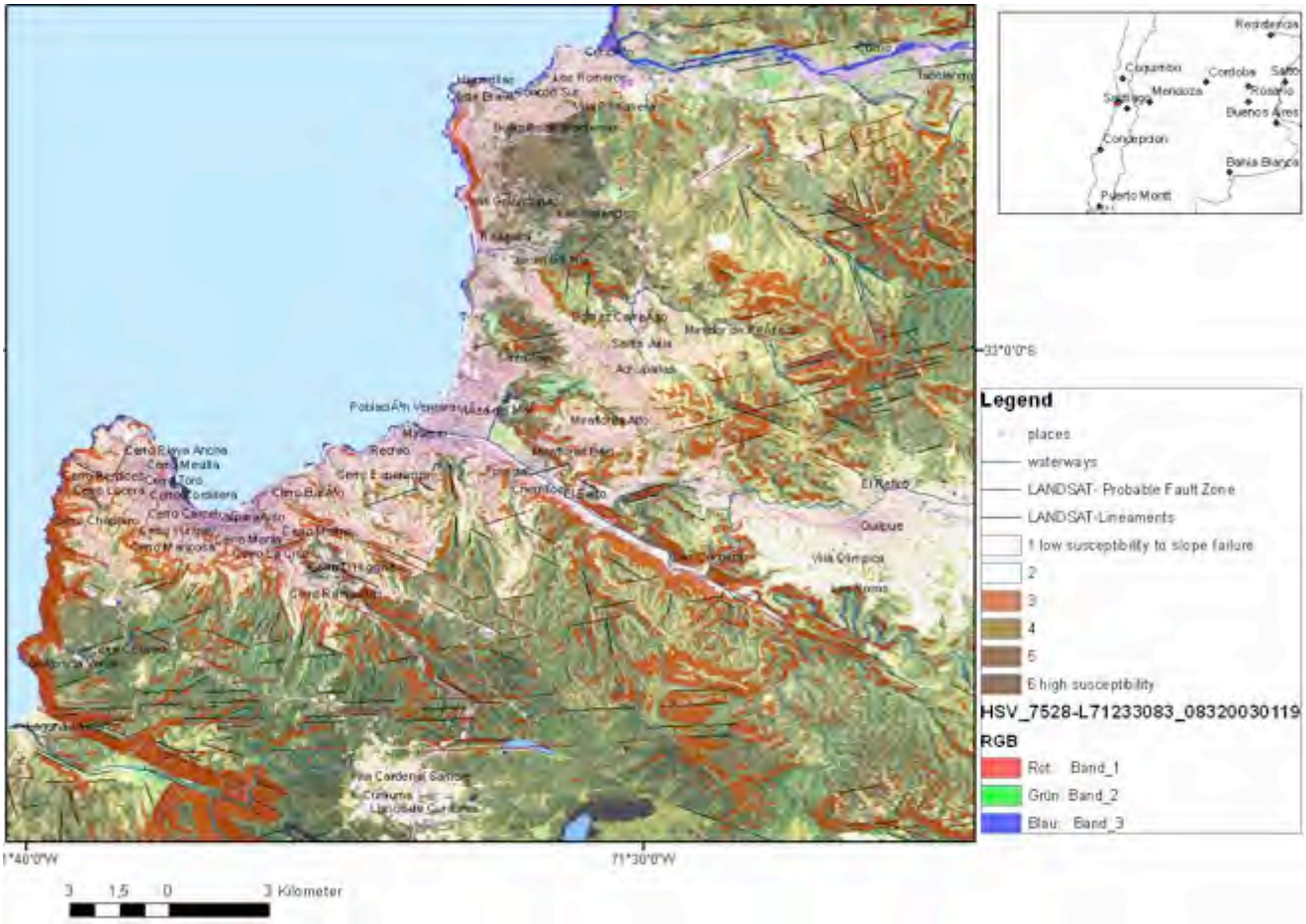

Figure 21: Weighted overlay calculation of some of the causal factors influencing slope stability based on ASTER DEM and LANDSAT data (weighted overlay of: [slope degree >40°] + [maximum curvature > 150]+ [height level > 500 m] + [fault zones-Grid]) and merging the weighted overlay results with LANDSAT data

The susceptibility to slope failure is assumed to be higher in areas of intersecting lineaments.
This approach of landslide susceptibility mapping is valid for a generalized assessment purpose. However, it is less useful on the site-specific scale, where local geological and geomorphologic heterogeneities prevail. Nevertheless this approach contributes to a better overview and understanding of the relationships between the different causal factors and helps to prepare more detailed investigations in the field.

8. CONCLUSIONS

The nearly world-wide available SRTM and ASTER-DEM data and LANDSAT imageries support a standardized, low-cost to no cost approach for the detection of some of the near-surface, causal factors of local site conditions influencing earthquake shock and damage intensity, as well as of factors influencing earthquake related secondary effects. A standardized procedure for mapping and assessing earthquake damage susceptibility has been developed based on the weighted overlay-approach, which can serve to improve the efficiency of disaster monitoring, management and preparedness. This approach integrates many types of data and geo-processing tools that can automate the processes in an efficient manner. Aggregating factors influencing the surface-near earthquake ground motion in a GIS environment allows a first overview of areas with probably higher susceptibility to soil amplification, slope failure and flooding. The advantage of GIS is that the system is open and additional data can be integrated as layers as soon as additional data are available. Thus, remote sensing data and GIS integrated evaluations and analysis can contribute to a better planning of cost and time-intensive geotechnical measurements that are important to consider. The derived results from the whole process provide essential information for immediate response when future disasters will occur.

Acknowledgements

The support of EU, FP 7, Large Collaborative Research Project, IRIS - Integrated European Industrial Risk Reduction System, CP-IP 213968-2, is kindly acknowledged.

REFERENCES

Allen, T. & Wald, D.: On the Use of High-Resolution Topographic Data as Proxy for Seismic Site Conditions (V_{S30}), Bulletin of the Seismological Society of America*;* April 2009; v. 99; no. 2A; p. 935-943,2009. DOI: 10.1785/0120080255

Calais, E., Mazabraud, Y., de Le´pinay, M.B., Mann, P., Mattioli, G. and Jansma, P.: Strain partitioning and fault slip rates in the northeastern Caribbean from GPS measurements, Geophysical Research Letters, VOL. 29, No. 18, 1856, doi:10.1029/2002GL015397, 2002.

Dolan, J., and Wald, D.: The 1943–1953 northcentral Caribbean earthquakes: Active tectonic setting, seismic hazards, and implications for Caribbean-North America plate motions, in Active Strike-slip and Collisional Tectonics of the Northern Caribbean Plate Boundary Zone*,* edited by J. Dolan and P.Mann, Geol. Soc.Am.Spec.Pap. 326, pp.143–169, Geological Society of America, Boulder, 1998.

Ehret, D.& Hannich, D.: Seismic Microzonation based on Geotechnical Parameters – Estimation of Site Effects in Bucharest (Romania). EOS Trans. AGU, 85 (47), Fall Meet. Suppl., Abstract S43A-0972; San Francisco, 2004.

Ehret, D. ; Kienzle, A. ; Hannich, D. ; Wirth, W. ; Rohn, J. ; Czurda, C.: Seismic microzonation based on geotechnical parameters - estimation of site effects in Bucharest (Romania). In: *Geophysical Research Abstracts; European Geosciences Union* 6 (2004), Nr. 6, S. 3708-3709

Hannich, D., Hötzl, H. & Cudmani, R.: Einfluss des Grundwassers auf die Schadenswirkung von Erdbeben – ein Überblick. Grundwasser,Vol.11,4, 286- 294,2006.

Giardini, D.,Wiemer S., Fäh D. & Deichmann, N.: Seismic Hazard Assessment of Switzerland,2004.- Swiss Seismological Service, ETH Zürich, Zürich, Switzerland,2004.

Gupta, R.P.: Remote Sensing in Geology, Springer-Verlag, Berlin- Heidelberg-New York, 2003.

Madariaga, R., Métois, M., Vigny, C. & Campos, J. (2010): Central Chile Finally Breaks.- SCIENCE, Vol. 328, 9, APRIL 2010, 181-182

Pararas-Carayannis, G. (2010): The Earthquake and Tsunami of 27 FEBRUARY 2010 in Chile –Evaluation of Source Mechanism and of Near and Far-field Tsunami Effects.- Science of Tsunami Hazards, Vol. 29, No. 2, 96-126

Schneider, G.: Erdbeben- Eine Einführung für Geowissenschaftler und Bauingenieure, Spektrum Akademischer Verlag, München,2004.

SHOA Report "CARTA DE INUNDACION POR TSUNAMI PARA LA BAHIA DE VALPARAISO, CHILE". http://www.shoa.cl/servicios/citsu/citsu.php

Sobiesiak, M. (2004): Fault Plane Structure of the 1995 Antofagasta Earthquake (Chile) Derived From Local Seismological Parameters.- Dissertation, University of Potsdam

Steinwachs M.(1988). Das Erdbeben am 19.September 1985 in Mexiko –Ingenieurseismologische Aspekte eines multiplen Subduktionsbebens, in: Steinwachs M. (ed).: Ausbreitungen von Erschütterungen im Boden und Bauwerk. 3.Jt. DGEB, TransTech.Publications, Claustha1,1988.

Theilen-Willige, B. and Wenzel, H.: Local Site Conditions influencing Earthquake Shaking Intensities and Earthquake related Secondary Effects - A Standardized Approach for the Detection of Potentially Affected Areas using Remote Sensing and GIS-Methods.- 10.Forum Katastrophenvorsorge, Katastrophen – Datenhintergrund und Informationen UN Campus, Bonn, 23. - 24. November 2009. http://188.111.81.194/download/forum/10/Theilen-Willige_Wenzel_ExtAbst.pdf

Theilen-Willige, B., Mulyasari Sule, F.& Wenzel H.: Environmental Factors derived from Satellite Data of Java, Indonesia, in: Christian Boller, Fu-Kuo Chang & Jozo Fujino (Editors): Encyclopedia of Structural Health Monitoring.- John Wiley and Sons,Ltd., Chichester,UK, 2343-2354, 2008.
http://www.jsg.utexas.edu/news/pdfs/011310/Tuttle_et_al_2003_DR.pdf

Wald, D.J. & Allen, T.I.: Topographic Slope as a Proxy for Seismic Site Conditions and Amplification.- Bulletin of the Seismological Society of America, October 2007; v. 97; no. 5; p. 1379-1395,2007. DOI: 10.1785/0120060267

Winckler Grez,P. & Vásquez Álvarez, J. (2008): Evaluacion de Riesgo de Tsunami en Quintero, Chile.-Anales del Instituto de Ingeniería de Chile. DOC ICO 01-2008**,** Vol 120 No 1, Abril 2008, 1-12 (ISSN 0716-2340), www.ingenieriaoceanica.cl/files/200801_**tsunami**_sochid2.pdf

Vigny, C., Rudloff, A., Ruegg, J.-C., Madariaga, R., Camposc, J., & Alvarezc, M.(2009): Upper plate deformation measured by GPS in the Coquimbo Gap, Chile.- Physics of the Earth and Planetary Interiors, 175 (2009), 86–95

Internet sources:

UNOSAT:
http://www.disasterscharter.org/image/journal/article.jpg?img_id=63885&t=1263988941535
USGS, Seismic Hazard Program, Global V_s^{30} Map Server
http://earthquake.usgs.gov/hazards/apps/vs30/
Southern California Earthquake Center, http://www.scec.org/phase3/overview.html
http://earthquake.usgs.gov/earthquakes/shakemap/background.php#accmaps
Earthquake and Tsunami Data free of Charge:
Centro Regional de Sismología para América del Sur (CERESIS), Catálogo de Intensidades, http://www.ceresis.org/producto/inten_ch.htm,
http://www.ceresis.org/portal/serie_sisra.php
NOAA's Satellite and Information Service (NESDIS)
http://www.ngdc.noaa.gov/hazard/data/publications/Wdcse-39.pdf and
Servicio Hidrografico y Oceanografico de la Armada de Chile,
http://www.shoa.cl/servicios/citsu/citsu.php).
BGR, Hannover:
http://www.bgr.bund.de/cln_145/nn_333452/DE/Themen/Seismologie/Seismologie/Erdbebenauswertung/Erdbebenkataloge/Kataloge__Bulletins/kataloge__bulletins__node.html?__nnn=true
LGRB, Freiburg:
http://www.lgrb.uni-freiburg.de/lgrb/Fachbereiche/erdbebendienst
SED - Swiss Seismological Service
International Seismological Centre, http://www.isc.ac.uk/search/custom/index.html
Stress Data of the WSM, http://dc-app3-14.gfz-potsdam.de/pub/stress_data/stress_data_frame.html

http://map.ngdc.noaa.gov/website/seg/hazards/viewer.htm
GFZ Potsdam GEOFON
http://geofon.gfz-potsdam.de/geofon/

Satellite Data free of Charge:

Global Land Cover Facility, University of Maryland:
http://glcfapp.glcf.umd.edu:8080/esdi/index.jsp
NASA: https://zulu.ssc.nasa.gov/mrsid/mrsid.pl

Digital Elevation Data free of Charge:

http://srtm.csi.cgiar.org/SELECTION/inputCoord.asp
http://glcfapp.glcf.umd.edu:8080/esdi/index.jsp
http://www.gdem.aster.ersdac.or.jp/search.jsp